CO_2 seawater acidification by CCS-simulated leakage: Kinetic modelling of Zn, Pb, Cd, Ni, Cr, Cu and As release from contaminated estuarine sediment using pH-static leaching tests

M.Camino Martín-Torre*, Gema Ruiz, Berta Galán, Javier R. Viguri

Green Engineering & Resources Research Group (GER), Department of Chemistry and Process & Resources Engineering, ETSIIT, University of Cantabria, Avda. de los Castros s/n, 39005 Santander, Cantabria, Spain

* Corresponding author. Tel.: +34 942 201583; fax: +34 942 206706

E-mail address: martinmc@unican.es (M.C. Martín-Torre)

Highlights

- Kinetic element release in a pH-static leaching test using CO_2 for acidification
- The model fits experimental release including the influence of Fe and other ions
- There is a leaching simulation over time under acidic scenarios up to pH=6
- CO_2 and HNO_3 acidifications lead to different kinetics during element release
- The generalised model proposed here is also useful for areas contaminated by iron

Keywords: Kinetic modelling; CO_2 acidification; contaminant release; sediment; pH-static leaching; Fe influence

Abstract

A modified pH-dependent leaching test with continuous pH control that employed CO_2 to acidify a seawater-sediment mixture is used to address Zn, Pb, Cd, Ni, Cr, Cu and As release from contaminated estuarine sediments under the influence of acidification

processes. Long-term (480 h) leaching experiments at pH values of 7.0, 6.5 and 6.0 are performed. The different evolutionary patterns of the redox potential and Fe release at pH=6 with respect to the other pH values shows the need to assess the influence of the initial Fe content in seawater upon elemental release.

Hence, assays at pH=6.0 are conducted using natural seawater with Fe concentrations between 9.02 and 153 μg/L. A set of in-series reactions for trace elements, Fe and other ions associated with Fe is proposed to model a Fe/multi-ion-dependent mechanism for trace metal release. The maximum concentration of each contaminant that can be released from the sediment and the kinetic parameters of the proposed model are completed for the studied pH values, for good consistency between the experimental and simulated mobilisation of each studied element.

1. INTRODUCTION

Carbon capture and storage (CCS) in geological formations is one of the most promising strategies for curbing global climate change (IPCC, 2014). One of the primary risks in the case of ocean storage technology is the potential direct leakage of CO_2 gas or CO_2 dissolved in seawater, which provokes a decrease in the pH of the medium. This acidification might mobilise contaminants from marine and estuarine sediments (Rodríguez-Romero et al., 2014; Ardelan et al., 2009).

Laboratory leaching tests allow for the assessment of contaminant releases under different scenarios and conditions. Column leaching tests (Bateman et al., 2005; Frye et al., 2012; Lawter et al., 2016; Payán et al., 2012a) and batch or semi-batch leaching

54 tests (Ardelan and Steinnes, 2010; Ardelan et al., 2009; de Orte et al., 2014; Kirsch et
55 al., 2014; Little and Jackson, 2010; Lu et al., 2010; Payán et al., 2012b) have been
56 performed to assess elemental mobilisation from different types of matrices such as
57 sediments, sandstones or rocks when the addition of CO_2 decreases the pH of the
58 medium.
59
60 The release of experimental contaminants from sediments and rocks by using different
61 leaching tests to mimic the effects of potential CO_2 leakages has been studied before.
62 Equilibrium conditions have been modelled using geochemical software such as
63 PHREEQC or Visual MINTEQ (de Orte et al., 2014a; Martín-Torre et al., 2015a),
64 whereas simulations for the period before equilibrium is achieved have been performed
65 using reactive transport models as performed with the TOUGHREACT code (Zheng et
66 al., 2016; Zheng et al., 2009) or PHREEQC (Cahill and Jakobsen, 2015).
67
68 Reactive transport models combine mineral dissolution/precipitation, aqueous
69 complexation, acid-base, redox, cation exchange and surface complexation processes.
70 Therefore, the use of this type of models for simulating contaminant mobilisation
71 implies that the modelled has knowledge of the different characteristics of the solid
72 matrix under study, such as crystalline phases, that are usually not possible to know in
73 the case of sediments because of their great complexity and low contaminant
74 concentrations. Moreover, the need to pre-treat the sediment sample complicates the
75 determination of element speciation in a sensitive manner.
76
77 The pH is one of the variables that most influences the mobility and availability of
78 inorganic contaminants from solid matrices (Coz et al., 2007), and thus, pH-dependent

leaching tests seem to be an appropriate assay for assessing its influence. Standard or modified pH-dependent leaching tests with continuous pH control such as CEN/TS 14997 (2015) have been widely used to evaluate the release of contaminants from soil and sediments (Cappuyns and Swennen, 2005; Cappuyns et al 2004a,b; Centioli et al., 2008; Horckmans et al., 2007; Shtiza et al., 2009; Van Herreweghe et al., 2002).

To study the release of contaminants that occurs when environmental conditions in marine and estuarine media vary, a modified pH-dependent leaching test with continuous pH control has been previously performed to assess the contaminants released from contaminated sediment when a total mixture of sediment-seawater is acidified by nitric acid (HNO_3) (Martín-Torre et al., 2015b). Based on these experimental results, a kinetic mathematical model has been proposed to obtain the generalised kinetic constants of the studied elemental release. Owing to the experimental difficulties involved in characterising the sediment and the many chemical reactions that occurred during the process, global phenomena rather than specific reactions have been considered.

It is known that inorganic contaminants, primarily metals and metalloids, are largely affected by acidification processes (Basallote et al., 2014), and that their effects on marine organisms are higher when using CO_2 gas than mineral acids (Ishimatsu et al., 2004; Kikkawa et al., 2004). Hence, the performance of a pH-dependent leaching test with CO_2 gas for acidification and the subsequent assessment and modelling of the triggered contaminant mobilisation from sediment would be useful for a CCS technology impact assessment.

104 The aim of the present work is to obtain, analyse and simulate the experimental release
105 of Zn, Pb, Cd, Ni, Cr, Cu and As from contaminated marine sediments during the pH-
106 static leaching test with continuous pH control by using seawater as a leaching liquid
107 and CO_2 gas to acidify the medium. The kinetic behaviour of Zn, Pb, Cd, Ni, Cr, Cu
108 and As is studied by using long-term experiments lasting 480 hours at pH values of 7.0,
109 6.5 and 6.0. The influence of the Fe content of the seawater on the redox potential
110 evolution and elemental release is highlighted at pH=6.0 because of the different
111 evolution of these parameters with respect to the experimental data obtained at pH
112 values of 7.0 and 6.5.
113
114 Starting with the mathematical model by Martín-Torre et al. (2015b) in which HNO_3
115 acidification was initially proposed, a modified kinetic model is proposed here to
116 explain the behaviour of long-term experimental data at different pH values and
117 different Fe concentrations in seawater. The generalised kinetic expression and its
118 kinetic parameters are obtained to fit the experimental and modelled release of the
119 elements.
120
121
122 **2. MATERIALS AND METHODS**
123 The selected estuarine sediment samples were collected in the Suances estuary
124 (Cantabrian region, northern Spain), which is a representative area for a possible CCS
125 (BOE, 2008). As explained in detail in Martín-Torre et al. (2015b), surface sediment (0-
126 5 cm) and its initial water content was collected using a plastic paddle, and it was sieved
127 through a 2 mm plastic mesh to remove the gravel fraction. Afterwards, the sediment
128 was homogenised and frozen in plastic bags until use.

129 An X-ray diffraction analysis (Siemens D5000 diffractometer) using Cu Kα radiation
130 and operating at 30 mA and 50 kV was used to determine the crystalline phases of the
131 selected sediment (Payán et al. 2012b). The total sediment content was determined by
132 an external laboratory (Activation Laboratories, Canada). The As and Cr contents were
133 measured by Instrumental Neutron Activation Analysis (INAA) and the Cd, Cu, Ni, Pb
134 and Zn contents were analysed by Total Digestion-Inductively Coupled Plasma/ Optical
135 Emission Spectrometry (TD-ICP/OES) method.

136

137 The results of the sediment characterisation are explained in more detail in Martín-Torre
138 et al. (2015b), but they are described briefly in Table 1.

139 Table 1. Principal crystalline phases, redox potential and trace element concentrations of the studied
140 sediment

Principal crystalline phases	Trace element	Content (mg/kg)
Quartz	Zn	5220 ± 140
Aluminium oxide	Pb	564 ± 2.22
Calcite	Cd	12.6 ± 0.732
Dolomite	Ni	36 ± 1.86
	Cu	48 ± 3.43
	Cr	72 ± 5.31
	As	59 ± 1.39
Redox potential (mV): -150±37		

141

142 The entire Cantabrian region and the Suances estuary in particular was an important
143 mining area, with a considerable number of iron ore mines and abandoned landfills
144 containing solid mining wastes. Therefore, the presence of this metal in rivers and
145 effluents that lead in the estuary and its accumulation in sediment is appreciable.
146 Therefore, the concentration of iron in the area from which the seawater is taken should
147 be influenced by tides and other atmospheric conditions. To prevent large variations in
148 the concentration determinations, the seawater was chemically analysed by using

149 inductively coupled plasma-mass spectrometry (ICP-MS) equipment in helium collision
150 mode according to the same procedure that was used for the sample leachates, prior to
151 use. Table 2 lists the average elemental concentrations in the seawater that was used in
152 the leaching assays at pH=7.0, 6.5 and 6.0. Seawater samples with iron concentrations
153 ($[Fe]_{seawater}$) of 9.02, 46.1 and 153 µg/L were sampled at the same place that the
154 sediment was taken from but under different natural conditions of tide, meteorology and
155 season.

156 Table 2. Concentration of the studied elements and redox potential in the seawater leachant

157

Element	Content (µg/L)
As	2.58±0.981
Cd	0.204±0.0797
Cr	0.920±0.631
Cu	2.46±1.49
Ni	1.21±1.37
Pb	0.929±0.727
Zn	11.6±8.21
Fe	6.45±2.91
Redox potential (mV)	160±16.0

158
159
160 The experimental equipment consisted of a glass-made 2-L jacketed vessel, a
161 temperature controller (Polyscience) and a system for maintaining a constant pH (Fig.
162 1). In this study, a pH controller (AT Control systems) with an electrode that was
163 suitable for samples containing suspended solids was used; it was accurate to 0.01 pH
164 units and was calibrated against standard solutions. This device was used to monitor the
165 pH and inject pure CO_2 bubbles into the suspension as needed, with a permitted
166 hysteresis of 0.1 pH units. When the suspension reached the required pH, the gas supply
167 was automatically stopped.

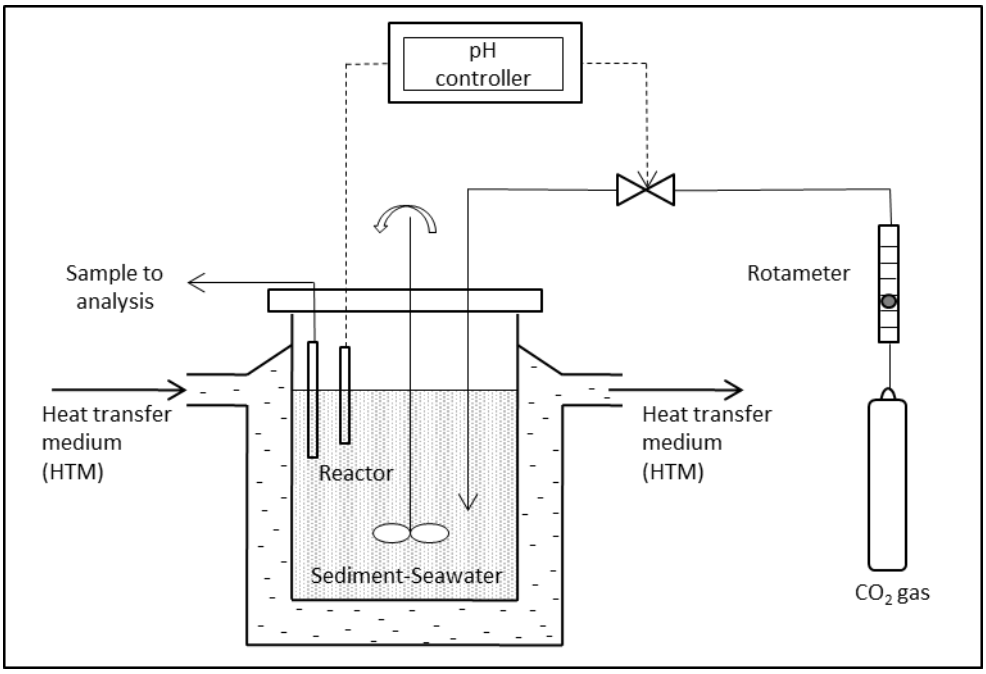

Fig. 1. Experimental equipment used in the pH-static leaching test with continuous pH control.

Seawater and sediment were placed in a reactor with an L/S ratio of 10, considering the moisture of the sediment (51.26%). To make a homogenised mixture at the beginning of the assay, the reactor was shaken for 15 minutes at the natural pH before starting the CO_2 addition (CO_2 supplied by AL Air Liquide España, S.A., Zamudio, Vizcaya, País Vasco, Spain). In this work, the studied pH values are 7.0, 6.5 and 6.0. It was not possible to achieve lower pH values because of the high buffering capacity of the sediment-seawater system (Martín-Torre et al., 2015a). Additionally, an assay without pH control was conducted to observe the pH evolution over time.

The pH-static leaching tests conducted in this work lasted almost 480 hours to achieve near-equilibrium conditions, which were not obtained over shorter assay durations (Martín-Torre et al., 2015b). Nevertheless, the assay at pH=7.0 lasts 264 hours, when the consumption of the buffer capacity of the mixture makes the pH uncontrollable. The experiments were performed in duplicate. Samples at 0, 0.5 h, 1 h, 3 h, 6 h, 12 h, 24 h,

48 h, 72 h, 96 h and afterwards for every 48 hours were taken using a syringe and without stopping the mixing. The redox potential (Eh) of the leachate was measured using a Basic 20 pH metre (Crison) with a special electrode for samples containing suspended solids; each sample was filtered through a 0.45-µm pore size nitrocellulose filtration membrane and acidified to determine the concentrations of Fe, Zn, Pb, Cd, Ni, Cr, Cu and As. The corresponding amount of solids was put back in the medium to maintain a constant L/S ratio during the whole assay.

The elemental concentrations were determined by an external laboratory (Mass Spectrometry Unit, University of Oviedo, Spain) using Agilent 7500CE inductively coupled plasma-mass spectrometry (ICP-MS) equipment in helium-collision mode (Agilent Technologies, California, EEUU). The samples were diluted (1:20) with HNO_3 (VWR International, Fontenay-sous-Bois, France) 1% prior to analysis, and Rh was added as an internal standard to correct for the eventual signal drift during analysis. The metal concentrations were calculated using external calibration with internal standard correction. The certified reference material NASS-5 (Seawater reference material for trace metals, NRCC (Ontario, Canada)) was spiked with the elements at two different concentration levels of 1 and 10 µg/L. The certified reference material and the two spiked concentrations were measured every 6 samples as a quality control. The detection limits for the elements under study (Fe, Zn, Pb, Cd, Ni, Cr, Cu and As) were 0.79; 0.75; 0.02; 0.06; 0.23; 0.03; 0.21 and 0.16 µg/L, respectively. Prior to the experiments, all the sampling and laboratory material was precleaned, acid-washed (10% HNO_3), and rinsed with Milli-Q water (Direct-Q 5 UV, Merck Millipore, USA).

209 The modelling of this study and the estimation of the corresponding parameters are
210 completed using Aspen Custom Modeler software (Bedford, Massachusetts, USA)
211 which solves rigorous models and simultaneously estimates parameters. The adjustment
212 of the model parameters was performed using an NL2SOL algorithm for the least-
213 square minimization of the deviation between the experimental and theoretical data.
214

215 ## 3. RESULTS

216 ### 3.1. Evolution of redox potential and Fe release at pH=7.0, 6.5 and 6.0

217 The evolution of the redox potential (E_h) over time is followed in all the assays. Similar
218 to the findings of Cappuyns and Swennen (2005), this evolution is as useful as the exact
219 values when considering that the measured value is a mixed redox potential. It cannot
220 be a true equilibrium potential because of the different redox couples in the sediment
221 and the slow kinetics of redox reactions (Sigg, 2000).
222

223 To compare the evolution of the redox potential at the different pH values under study
224 better, Fig. 2 shows the evolution of the redox variation (E_h- $E_{h,0}$) over time. During the
225 first 30-60 minutes of the assay there is a rapid increase in the E_h value, possibly
226 because of the dissolution of major ions from the sediment. After this initial increase, a
227 common trend is observed for pH=7.0 and 6.5. In these cases, the E_h value increases
228 from t=1 h until t=50-72 h. Afterwards, the value of this parameter remains almost
229 constant.
230

231 At pH=6.0 and the Fe concentration in the selected seawater ($[Fe]_{seawater}$) of 9.02 µg/L,
232 the E_h value shows an irregular and different time behaviour it decreases from 1 to 12
233 hours. Afterwards, it remains almost constant until 48 h, when a rapid increase begins.

After a maximum E_h of 96 h, a decrease occurs. There is a subsequent increase until 192 h, when it remains almost constant until the end of the assay.

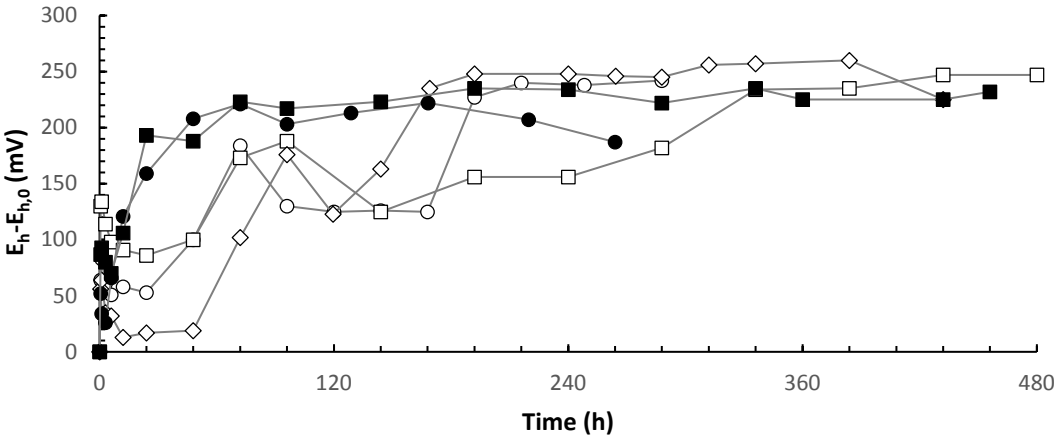

Fig. 2. Evolution of redox variation (mV) over time in pH-static leaching tests. $E_{h,0}$ and E_h are the redox potentials at t=0 h and t=t, respectively. ● pH=7; ■ pH=6.5; ◇pH=6.0, $[Fe]_{seawater}$=9.02 µg/L; ○ pH=6.0, $[Fe]_{seawater}$ =46.1 µg/L; and □ pH=6.0, $[Fe]_{seawater}$ =153 µg/L. Connecting lines were added for clarity.

As shown in Fig. 3 a and b, at pH values of 7.0 and 6.5, the dissolved Fe concentration increases during the first three hours because of the mixing of the wet sediment with the seawater and possibly because of the oxidation and later release of different iron compounds. Afterwards, there is a decrease in the dissolved Fe concentration as a consequence of the Fe(II) to Fe(III) oxidation and the subsequent precipitation of Fe(III), which is much less soluble than Fe(II). When Fe(III) precipitates, it might form various compounds such as Fe oxyhydroxides (Appelo et al., 1999; Wang et al., 2016). A minimum value of approximately 10 µg/L, which remains constant until the end of the assay, is achieved at t=24 h when the pH is 7.0 and at 96 hours at pH=6.5.

The release of Fe at pH=6.0 and $[Fe]_{seawater}$= 9.02 µg/L (Fig. 3 c) is higher than it is at more neutral pH values because of its higher solubility at lower pH values (Johnston et al., 2016). Moreover, the experimental results at pH=6.0 indicate that high concentrations of Fe remain dissolved until 48 hours of the assay has passed, most

likely because of the slower oxidation of Fe(II) to Fe(III) at pH=6.0. This finding is completely consistent with previous studies showing that the rate constant of Fe(II) oxidation increases at higher pH values as well as in the presence of HCO_3^- ions (Millero and Izaguirre, 1989; Millero et al., 1987). The concentration of HCO_3^- at pH values of 7.0 and 6.5 (0.90 and 0.82 molar fraction, respectively) is higher than it is at pH=6.0 (0.6 molar fraction) (Payán et al., 2013). In coinciding with the high increase of the E_h value from 48 to 96 h, the dissolved Fe concentration decreases because of its oxidation to Fe(III) and its subsequent precipitation. A low Fe release, from 40 to 60 µg/L, is maintained from t=192 h to the end of the assay. This final dissolved concentration is higher at pH=6.0 than at more neutral pH values, likely because of the increase ~~of~~ in the Fe solubility at lower pH values.

The different behaviour of both parameters (E_h and Fe release) at pH=6.0 leads us to assess the influence of the initial Fe concentration in the seawater on the elemental release and to consider it as an important variable in leaching tests at pH=6.0.

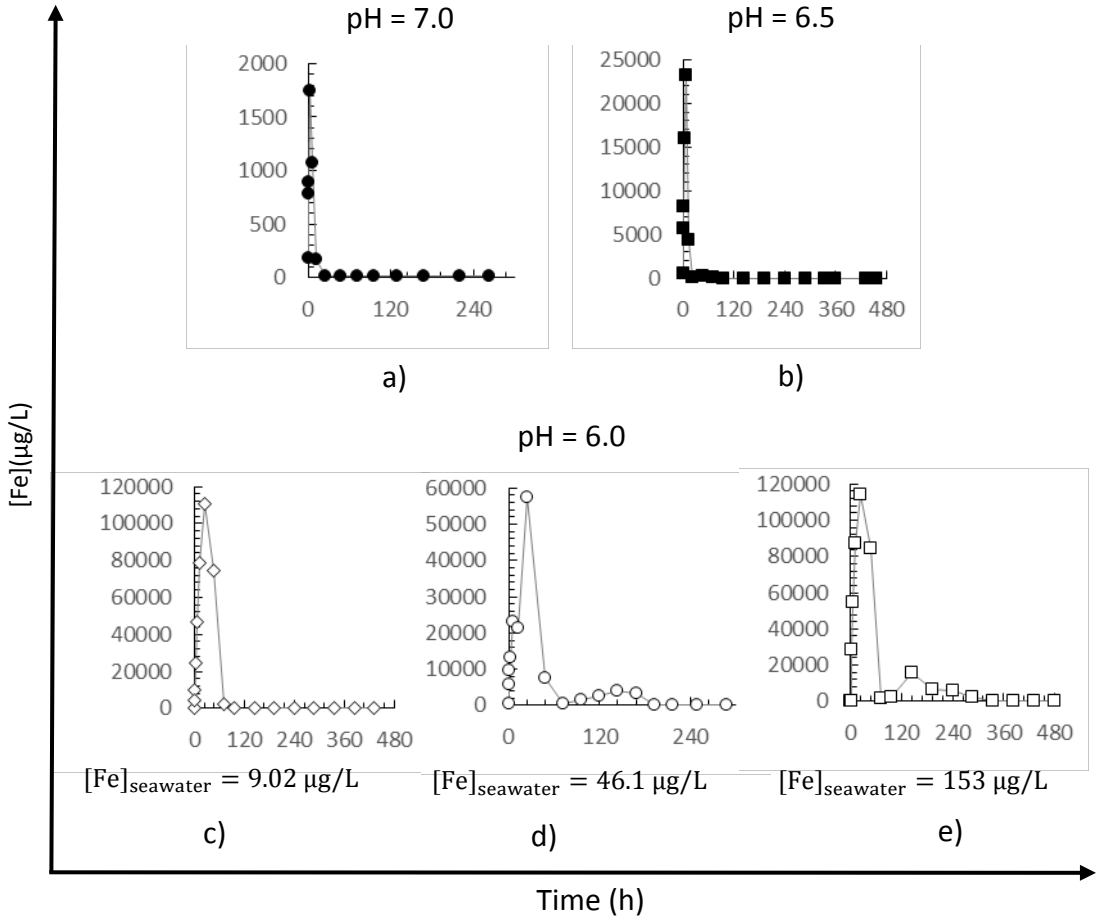

Fig. 3. Fe release (µg/L) over time in pH-static leaching tests: ● pH=7; ■ pH=6.5; ◇pH=6.0, $[Fe]_{seawater}$=9.02 µg/L; ○ pH=6.0, $[Fe]_{seawater}$=46.1 µg/L; and □ pH=6.0, $[Fe]_{seawater}$=153 µg/L. Connecting lines were added for clarity.

3.2. Evolution of redox potential and Fe release at pH=6.0 using seawater with different Fe content

In accounting for the fact that the Fe concentration of the selected seawater from the studied estuarine area fluctuates because of local tides and atmospheric conditions, assays at pH=6.0 are conducted using seawater with higher Fe concentrations, namely 46.1 and 153 µg/L, and lower E_h values of 61 and 116 mV, respectively. The concentrations of the other studied elements do not present as much variation, and they fall within the concentration range shown in Table 2.

In Fig. 2, the value of E_h increases in the assays conducted at pH=6.0 when using seawater with higher concentrations of Fe are also shown. During the first 24 hours of the assay, the evolution of the Eh of the three assays that were performed at pH=6.0 follows the same pattern: the increase during the first half hour is followed by a slight decrease and a plateau that lasts until 24 h when the $[Fe]_{seawater}$=46.1 µg/L or 48 hours in the other two cases. This difference might be more strongly influenced by the concentration of the major ions that are present in the seawater and the heterogeneity of the sediment rather than by the Fe content of the seawater. When the plateau ends, a rapid increase occurs until 72-96 h, depending on the experiment. At t=72 h and $[Fe]_{seawater}$= 46.1 µg/L, the E_h begins to decrease and a plateau is observed until t=168 h. At the lowest and highest $[Fe]_{seawater}$, the decrease begins at 96 h and it lasts from 96 to 144 h in the case of $[Fe]_{seawater}$=153 µg/L. Afterwards, there is an increase, which is less pronounced at higher Fe concentrations in the seawater, which ends in a constant value that is maintained until the end of the assay. The time at which the redox potential begins to remain constant seems to depend on the Fe content, because at the higher seawater Fe concentration, a constant E_h value is achieved later (192 h, 216 h and 432 h).

In all the assays conducted at pH=6, high Fe concentrations are in dissolution during the first 24 or 48 hours (Fig. 3 c, d and e). Afterwards, the precipitation of Fe(III) decreases the dissolved Fe concentration, and a minimum release is observed at 72 h ($[Fe]_{seawater}$ = 46.1 and 153 µg/L) or 96 h when $[Fe]_{seawater}$=9.02 µg/L. In assays with $[Fe]_{seawater}$ values of 46.1 and 153 µg/L, an increase in the Fe mobilisation is observed at 168 and 288 h, respectively; it is more pronounced at the highest Fe concentration in the initial seawater. Once the dissolved Fe concentration decreases after the second peak, likely

because of the Fe(II) oxidation and later precipitation of Fe(III), similar Fe release values are obtained at the end of the three assays that were performed at pH=6.0 (36.5±8.5 µg/L).

The fact that there is a second dissolved Fe concentration peak suggests a mobilisation that could be induced by different phenomena such as the destabilisation of Fe(III) oxyhydroxides or ionic competition and displacement reactions.

The destabilisation of Fe(III) oxyhydroxides could be caused by their reductive dissolution (Root et al., 2007). In this case, the abiotic reactions promoted by organic compounds present in the medium and H_2S might provoke this reductive dissolution (Hering and Stumm, 1990; Schwertmann, 1991; Thamdrup, 2000). Luther III et al. (1992) identify acidification as one of the different impacts that cause iron oxyhydroxides to become unstable. H_2S could be formed when Fe-sulphides are dissolved, and S^{2-} reacts with protons from the acidification (Cappuyns and Swennen, 2005). In the presence of sulphides, destabilised iron oxyhydroxides are converted into iron sulphides (Salomons, 1995; Luther III et al., 1992) that might be oxidised and released into the medium.

Iron monosulphides are partially soluble in water, with higher solubility at lower pH values, whereas other metal monosulphides are less soluble than Fe monosulphides. Hence, the displacement of Fe from monosulphides occurred as well as the inclusion of other divalent metals in iron monosulphides, as shown in Eqs. 1 and 2 respectively, could be the cause of an increase in the concentration of dissolved Fe^{2+} (Di Toro et al., 1990; Morse and Arakaki, 1993; Wong et al., 2013).

335

$$Fe_2S + Me^{2+} \rightarrow Fe(Me)S + Fe^{2+} \quad (1)$$

$$FeS + Me^{2+} \rightarrow MeS + Fe^{2+} \quad (2)$$

336

337 Ionic competition is a phenomenon that might be occurring constantly because of the
338 huge number of ions present in the medium, because seawater was used as well as the
339 acidification caused by CO_2 gas. In contrast to the assays at pH=6.0 with HNO_3 by
340 Martín-Torre et al. (2015b), in this study the displacement reactions might be an
341 important phenomenon because CO_2 gas was used to acidify the mixture. The use of
342 this gas instead of HNO_3 to acidify- the mixture affects the different equilibria present in
343 the suspension, and the newly formed ions could highly influence the release of the
344 studied contaminants (Tokoro et al., 2010).

345

346 **3.3. Trace element release**

347 The average value of the experimental results obtained for the release of Zn, Pb, Cd, Ni,
348 As, Cu and Cr from the pH-static leaching test and the error bars between both
349 replicates are shown in Fig. 4. The relative error between both replicates under the same
350 leaching conditions is lower than 20% for any of the studied contaminants. Moreover,
351 the relative error of more than 85% of the experimental data for Zn, Pb, Cd, Ni and As
352 is lower than 10%. Most of the experimental data from the Cr and Cu release show
353 errors between 10% and 20%, likely as a consequence of their low mobilisation from
354 the sediment in any of the studied conditions. The release of Cr is lower than 2 µg/L and
355 does not present a clear trend over time. Something similar occurs in the case of Cu in
356 that its release does not indicate a clear pattern and its dissolved concentration is lower

than 10 µg/L in all of the studied scenarios with respect to the pH and Fe concentrations.

The release of Ni does not present any initial delay in any of the assays. Moreover, after an initial rapid release, a near-equilibrium condition is reached after 300 h of the assay at pH values of 7.0 and 6.5. It is necessary to extend the experiment from 432-480 h to reach this condition in assays that were conducted pH=6.0. As shown here, in comparing the three assays at this most acidic pH value, lower Fe concentrations in seawater cause a faster mobilisation of Ni as well as a higher dissolved Ni concentration under the near-equilibrium condition.

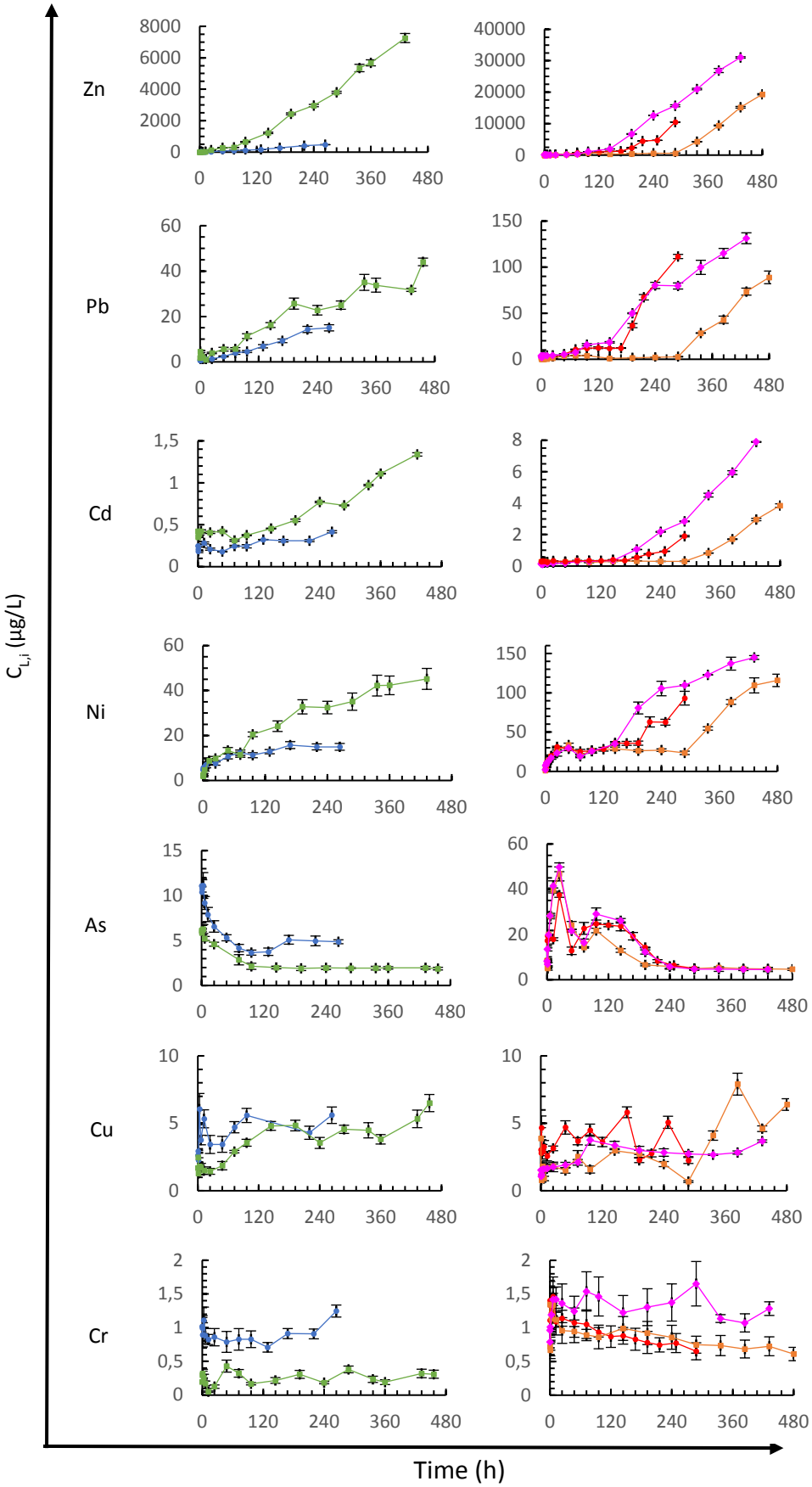

Fig. 4. Elemental release over time in all assays. • pH=7.0; ■ pH=6.5; ◆ pH=6.0, $[Fe]_{seawater}$=9.02 µg/L; ● pH=6.0, $[Fe]_{seawater}$=46.1 µg/L; and ■ pH=6.0, $[Fe]_{seawater}$=153 µg/L. Connecting lines were added for clarity. Error bars are also shown.

Regarding Cd, Pb and Zn mobilisation, an initial delay is observed that might be the consequence of the association of these metals with sulphur and the slow oxidation kinetics of these metal sulphides during the assay (Cappuyns and Swennen, 2008; Ho et al., 2012). This finding is supported by the evolution of the pH over time in the assay without pH control as shown in Fig. 5. Without CO_2 addition, the acidification of the medium that was observed during the first 65 h of assay, might be caused by the H^+ released from the oxidation reactions of reduced compounds such as sulphides (Cappuyns and Swennen, 2005; Eggleton and Thomas, 2004; Hwang et al., 2011). At pH=6.0, higher concentrations of Fe in the seawater cause longer delays in the release of these metals as a consequence of the higher solubility of Fe monosulphides than the cation monosulphides, which favours the precipitation of dissolved metal ions (Di Toro et al., 1990; Morse and Arakaki, 1993) at the same time that Fe^{2+} is released (Eq. 1 and 2). Moreover, the delay caused by the different solubility products might also be influenced by ionic competition to form compounds with other ions in the medium, such as CO_3^{2-}, SO_4^{2-} or Cl^- (Millero, 2009; Millero et al., 1995; Wong et al., 2013).

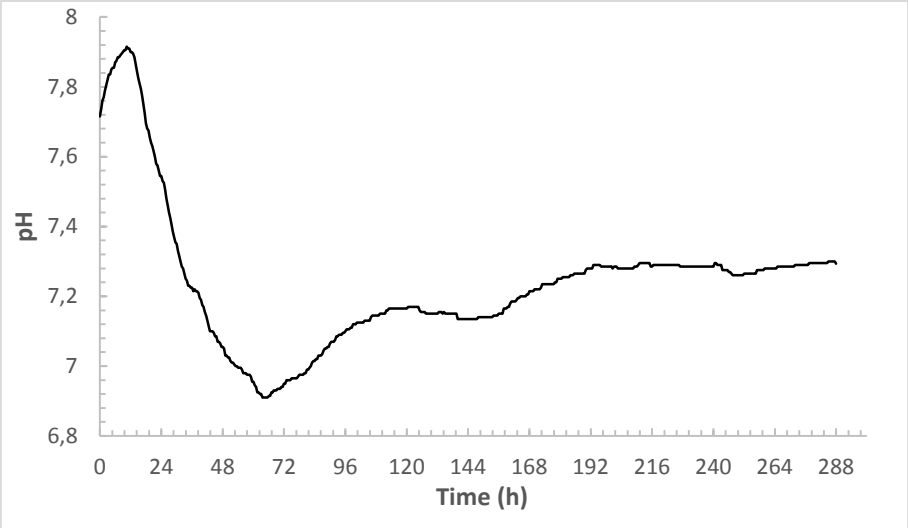

Fig. 5. pH evolution over time in the leaching test without pH control.

After an initial rapid release of As from the sediment, which became more pronounced at more neutral pH values, there is a decrease in the As concentration. The removal of this element from the solution has been widely believed to be caused by the coprecipitation and adsorption provoked by the production of iron oxyhydroxides (Cappuyns et al., 2005; Omoregie et al., 2013; Wallmann et al., 1996; Zhang et al., 2007); therefore, the oxidation rate of Fe(II) highly influences the time over which the oxyanion As remains in solution. Hence, at the most acidic pH value in the study, the presence of dissolved As is longer than that of the other two pH values under study. Moreover, As precipitation as trace metal arsenates represents a potential mechanism that contributes to this decrease (Vaca-Escobar et al., 2015). In the case of pH=6.0, after a minimum dissolved concentration of approximately 48-72 h, the mobilisation of As increases. This mobilisation might be a consequence of the destabilisation of Fe(III) oxyhydroxides, and the As might be adsorbed. The lower adsorbing capacity of iron sulphides, which are formed with the destabilisation of Fe(III) oxyhydroxides, causes an increase in the dissolved As concentration (Salomons, 1995). Moreover, sorbed As could be released after being displaced by the action of other oxyacids such as

412 phosphate, sulphate, carbonate, bicarbonate and silicate (Appelo et al., 2002; Arai et al.,
413 2014; Jain and Loppert, 2000; Meng et al., 2002, 2000).
414
415 **4. MODELLING AND DISCUSSION**
416 The pH-static leaching test used here allows for the study of elemental release from
417 contaminated sediment as a function of pH and time. Modelling the obtained
418 experimental results is useful for assessing the evolution of contaminant over time at the
419 pH values of interest.
420
421 Owing to the impossibility of performing a rigorous characterisation of all the species
422 present in the sediment, the difficulties involved in analysing the major seawater ions
423 mobilised from the sediment and the high number of chemical reactions that occurred
424 during elemental release, simplified kinetic models that consider general reaction
425 schemes to interpret contaminant release from sediments are usually proposed (Martín-
426 Torre et al., 2015b).
427
428 Therefore, generalised mathematical models are useful for studying contaminant release
429 and for determining the principal processes that influence their mobilisation, without
430 specifying all the phenomena that occurred within the sediment. The proposed
431 mathematical model is not applied to the experimental results of Cu and Cr because
432 their release over time does not present a clear trend, and it is very low, at lower than 10
433 µg/L in all cases.
434
435 **4.1. Generalised kinetic model as applied to Zn, Pb, Cd, Ni, Cr, Cu and As**

The kinetic model proposed in Martín-Torre et al. (2015b) for HNO_3 acidification, is used here. This model considers that the contaminant (M) is associated with an oxidised fraction (MOx) and with a reduced fraction (MRed) of the sediment that must be oxidised before the release of the element. Moreover, it includes the adsorption or precipitation of the released element through a third reaction in series. The reaction scheme and mass balances, when considering first-order reactions, are shown in Eqs. 3-7.

$$\mathrm{MRed(s)} \xrightarrow{k_{1,i}} \mathrm{MOx(s)} \xrightarrow{k_{2,i}} \mathrm{M(aq)} \xrightarrow{k_{3,i}} \mathrm{M_{Ad}(s)} \quad (3)$$

$$\frac{d[MRed]_i}{dt} = -k_{1,i}\,[MRed]_i \quad (4)$$

$$\frac{d[MOx]_i}{dt} = k_{1,i}\,[MRed]_i - k_{2,i}\,[MOx]_i \quad (5)$$

$$\frac{d[M]_i}{dt} = k_{2,i}\,[MOx]_i - k_{3,i}\,[M]_i \quad (6)$$

$$\frac{d[MAd]_i}{dt} = k_{3,i}\,[M]_i \quad (7)$$

where $[MRed]_i$, $[MOx]_i$, $[M]_i$ and $[MAd]_i$ are the concentrations of element i in the reduced sediment fraction, the oxidised sediment fraction, the aqueous phase and in the adsorbed or precipitated phase, respectively. The $k_{j,i}$ are the rate coefficients of element i in reaction j (oxidation, release or adsorption/precipitation), and t is the reaction time.

The integral equation of the set from Eqs. 4-7 is shown in Eq. 8.

$$\frac{LS}{1000}\,[M]_i = \left(\frac{k_{1,i}\,k_{2,i}\,[MRed]_{i,0}}{(k_{2,i}-k_{1,i})\,(k_{3,i}-k_{1,i})}\right)\exp(-k_{1,i}t) + \left(\frac{k_{1,i}\,k_{2,i}\,[MRed]_{i,0}}{(k_{1,i}-k_{2,i})\,(k_{3,i}-k_{2,i})} - \frac{k_{2,i}\,[MOx]_{i,0}}{(k_{2,i}-k_{3,i})}\right)\exp(-k_{2,i}t) + \left(\frac{LS\,[M]_{i,0}}{1000} + \frac{k_{2,i}\,[MOx]_{i,0}}{(k_{2,i}-k_{3,i})} + \frac{k_{2,i}\,k_{1,i}\,[MRed]_{i,0}}{(k_{1,i}-k_{3,i})\,(k_{2,i}-k_{3,i})}\right)\exp(-k_{3,i}t) \quad (8)$$

where LS corresponds to the Liquid/Solid ratio of the experiment, $[M]_{i,0}$, which is expressed in units of μg/L, is the concentration of element i in the liquid at $t = 0$ and $[MRed]_{i,0}$ and $[MOx]_{i,0}$ are the maximum concentration as expressed in mg/kg, of element i that can be released from the reduced and oxidised fractions of the sediment respectively.

The resolution of the model implies the estimation of the rate coefficients and the initial concentrations of each contaminant i in the oxidised and reduced fractions ($[MOx]_{i,0}$ and $[MRed]_{i,0}$, respectively) based on the experimental results. The experimental and simulated results obtained at pH values of 7.0, 6.5 and 6 at $[Fe]_{seawater}$=9.02 μg/L are shown in Fig. 6 and 7, and the initial concentrations are listed in Table 3. To better represent the elemental release, a dimensionless quotient (Eqs. 9-10) is represented over time.

$$x_i = \frac{[M]_i - [M]_{i,0}}{\frac{[MS]_{i,0}}{LS}} \quad (9)$$

$$[MS]_{i,0} = [MOx]_{i,0} + [MRed]_{i,0} \quad (10)$$

where $[M]_i$ is the dissolved concentration of the element i at any time (in units of µg/L), $[M]_{i,0}$ is the dissolved concentration of the element i at $t = 0$ (in units of µg/L), $[MRed]_{i,0}$ and $[MOx]_{i,0}$ are the maximum concentrations of the element i that can be leached from the reduced and oxidised fractions of the sediment, respectively (in units of mg/kg), $[MS]_{i,0}$ is the maximum concentration of element i that can be released from the sediment (in units of mg/kg) and LS is the Liquid/Solid ratio of the experiment (in L/kg).

Higher concentrations are released from the reduced fraction than from the oxidised fraction, except in the case of Ni, because of the initial reduced state of the sediment. In the case of Cd, its concentration in the oxidised fraction is zero.

Table 4 lists the kinetic rate coefficients of the reactions ($k_{j,i}$). According to the experimental results obtained here, the third adsorption or precipitation reaction is only included in the case of As. For the pH values under study, a good fit between experimental and simulated release concentrations is indicated by the percentage variation-explained values (R^2) of 99.4 (pH =7.0), 99.6 (pH = 6.5) and 98.3 (pH = 6.0 and $[Fe]_{seawater}$=9.02 µg/L).

Using the model published in Martín-Torre et al. (2015b), the simulated results for Zn, Pb, Cd, Ni and As fit more poorly with the experimental data at pH=6.0 than at the higher pH values, as shown in Fig. 7 with dashed lines for the three assays at this pH value. Among the different assays at pH=6.0, the better fit is obtained at the lowest concentration of seawater Fe (9.02 µg/L), and it seems that the initial concentration of

Fe in the seawater highly influences the characteristics of the medium, modifying the release behaviour of the contaminants. The experimental release of Zn, Pb and Cd at pH=6.0 present a longer delay than that simulated with this model. This delay in the release could be a consequence of the displacement reactions because of the higher solubility of the Fe(II) compounds at the most acidic pH value under study. The studied trace elements, except As, present a rapid release once Fe is removed from the aqueous phase. Hence, a modified mathematical model that considers the initial Fe concentration, its release and its precipitation is proposed.

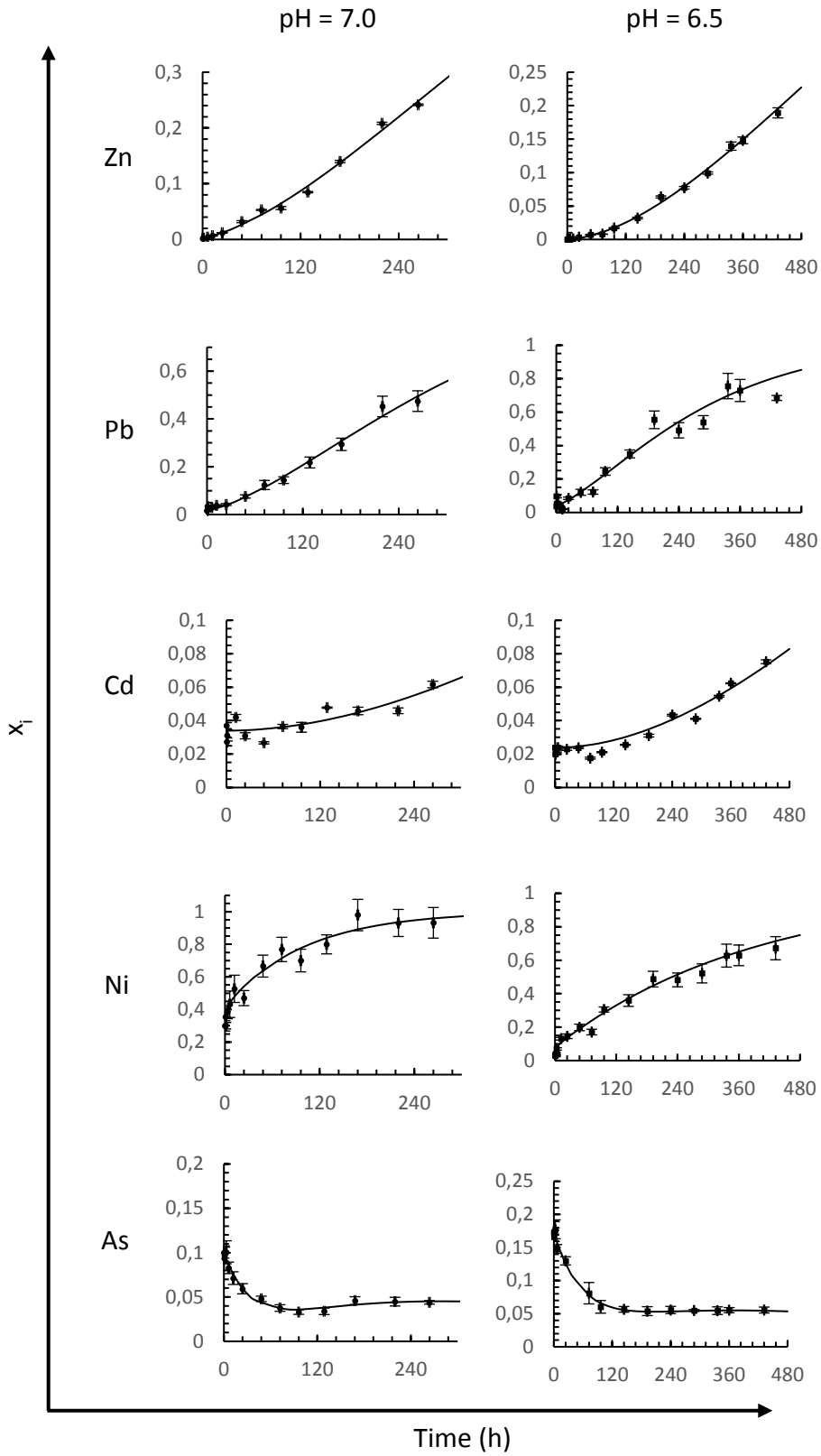

Fig. 6. Trace element release $x_i = \{[M]_i - [M]_{i,0}\}/\{[MS]_{i,0}/LS]\}$ over time at pH values of 7.0 and 6.5, where i is the trace element, $[M]_i$ is the dissolved concentration of the element i, $[M]_{i,0}$ is the dissolved concentration of the element i at $t = 0$ and $[MS]_{i,0}$ i is the maximum concentration of the element that can be released from the sediment. The experimental release (● pH=7; ■ pH=6.5), error bars and simulated curves using the model by Martín-Torre et al. (2015b) (—) are represented.

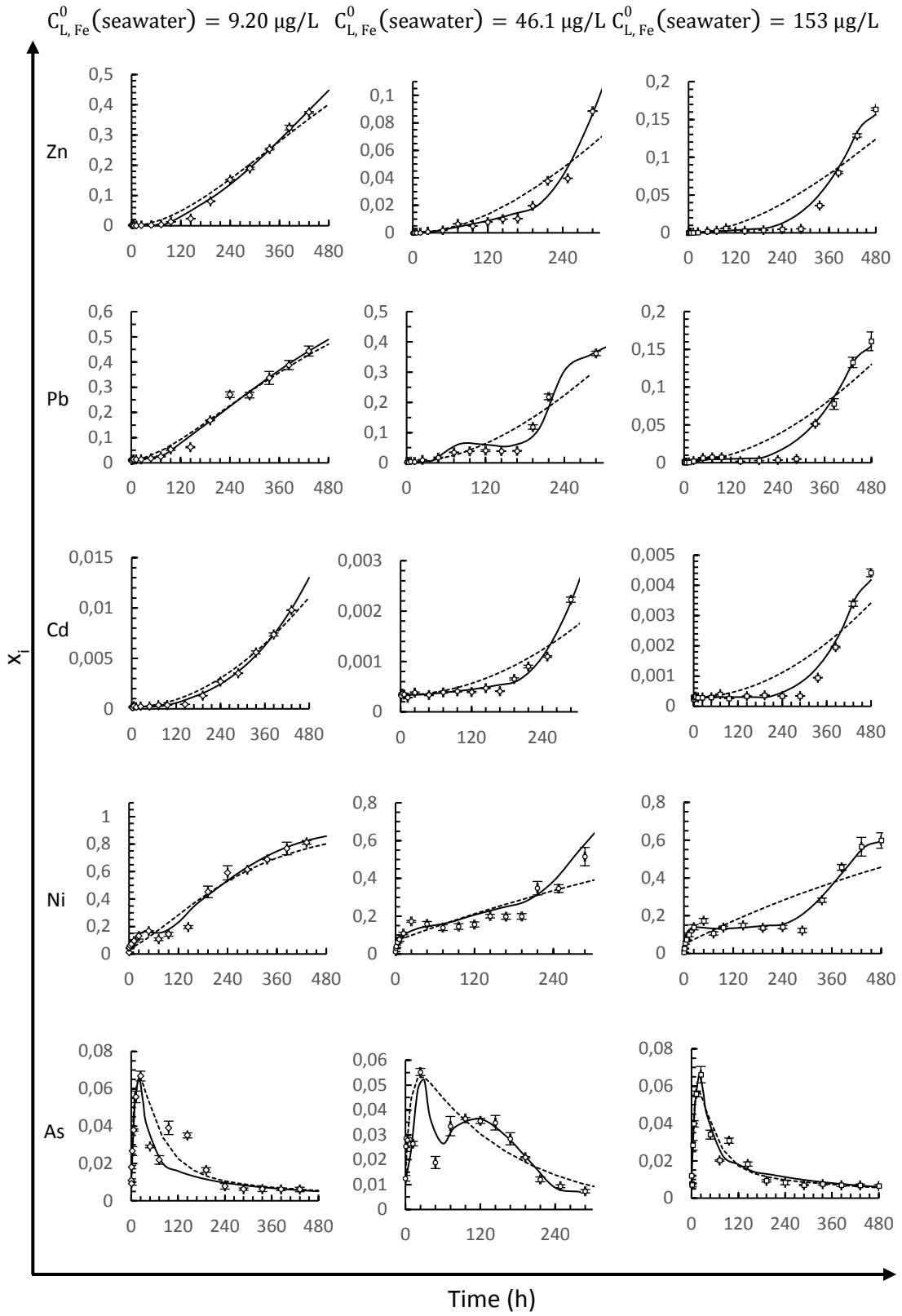

Fig. 7. Trace element release ($x_i = \{[M]_i - [M]_{i,0}\}/\{[MS]_{i,0}/LS]\}$) over time at pH=6.0, where i is the trace element, $[M]_i$ is the dissolved concentration of the element i, $[M]_{i,0}$ is the dissolved concentration of the element i at $t = 0$ and $[MS]_{i,0}$ i is the maximum concentration of the element that can be released from the sediment. Experimental release (◇pH=6.0, $[Fe]_{seawater}$=9.02 µg/L; ○ pH=6.0, $[Fe]_{seawater}$ =46.1 µg/L; and □ pH=6.0, $[Fe]_{seawater}$ =153 µg/L), error bars and simulated curves are represented: - - - Martín-Torre et al. (2015b) model; and ___ modified model

Table 3. Estimated values of the maximum concentrations that can be released from the reduced and oxidised fractions of the sediment, ($[MRed]_{i,0}$ and $[MOx]_{i,0}$ respectively), as expressed in units of mg/kg.

Assay		Contaminant									
pH	$[Fe]_{seawater}$ (µg/L)	Zn		Pb		Cd		Ni		As	
		$[ZnRed]_0$	$[ZnOx]_0$	$[PbRed]_0$	$[PbOx]_0$	$[CdRed]_0$	$[CdOx]_0$	$[NiRed]_0$	$[NiOx]_0$	$[AsRed]_0$	$[AsOx]_0$
Martín-Torre et al. (2015b) model											
7.0	6.80	17.6	2.06	0.280	0.0359	0.0676	0	0.0908	0.280	0.971	0.136
6.5	3.50	373	10.8	0.390	0.0733	0.178	0	0.635	0.390	0.298	0.0557
6.0*	9.02	828	0	2.96	0	8.06	0	1.14	2.96	5.01	2.43
Modified model for pH=6											
6.0	46.1	1150	33.9	3.07	0.012	8.53	0	1.65	3.07	4.37	7.70
6.0	153	1110	70.6	5.11	0.424	8.71	0	1.082	5.11	4.40	2.37

*Estimated concentrations at pH=6 and $[Fe]_{seawater}$=9.02 µg/L take the same value when using the model by Martín-Torre et al. (2015b) and the modified model at pH=6.

Table 4. Estimated kinetic rate coefficients for each contaminant in all the assays.

Assay			Contaminant				
pH	**$[Fe]_{seawater}$ (µg/L)**	**$k_{j,i}$ (h^{-1})**	**Zn**	**Pb**	**Cd**	**Ni**	**As**
Martín-Torre et al. (2015b) model							
7.0	6.80	$k_{1,i}$	$3.10\ 10^{-3}$	$5.02\ 10^{-3}$	$7.77\ 10^{-3}$	$9.95\ 10^{-3}$	$3.54\ 10^{-3}$
		$k_{2,i}$	$3.30\ 10^{-3}$	$6.34\ 10^{-3}$	$1.09\ 10^{-3}$	$3.06\ 10^{-3}$	$3.62\ 10^{-3}$
		$k_{3,i}$	0	0	0	0	$2.92\ 10^{-2}$
6.5	3.50	$k_{1,i}$	$1.96\ 10^{-3}$	$4.64\ 10^{-3}$	$6.41\ 10^{-3}$	$2.54\ 10^{-3}$	$2.08\ 10^{-3}$
		$k_{2,i}$	$1.70\ 10^{-3}$	$8.60\ 10^{-3}$	$1.04\ 10^{-3}$	$2.91\ 10^{-1}$	$2.86\ 10^{-3}$
		$k_{3,i}$	0	0	0	0	$1.64\ 10^{-2}$
6.0	9.02	$k_{1,i}$	$2.30\ 10^{-3}$	$1.60\ 10^{-3}$	$3.01\ 10^{-4}$	$7.69\ 10^{-3}$	$2.18\ 10^{-3}$
		$k_{2,i}$	$3.68\ 10^{-3}$	$1.09\ 10^{-3}$	$3.46\ 10^{-4}$	$5.88\ 10^{-3}$	$1.74\ 10^{-2}$
		$k_{3,i}$	0	0	0	0	$1.15\ 10^{-1}$
Modified model for pH=6							
6.0	9.02	$k_{1,i}$	$2.30\ 10^{-3}$	$1.60\ 10^{-3}$	$3.01\ 10^{-4}$	$7.69\ 10^{-3}$	$2.18\ 10^{-3}$
		$k_{2,i}$ $k^0_{2,i}$	$5.28\ 10^{-4}$	$4.36\ 10^{-3}$	$2.57\ 10^{-5}$	0	$1.14\ 10^{-2}$
		$k_{2,i}$ $k^1_{2,i}$	$1.74\ 10^{-5}$	$4.08\ 10^{-5}$	$1.65\ 10^{-6}$	$4.05\ 10^{-5}$	$2.34\ 10^{-3}$
		$k_{2,i}$ $k^2_{2,i}$	---	0	---	$2.03\ 10^{-3}$	0
		$k_{3,i}$	0	0	0	0	$1.15\ 10^{-1}$
6.0	46.1	$k_{1,i}$	$2.30\ 10^{-3}$	$1.60\ 10^{-3}$	$3.01\ 10^{-4}$	$7.69\ 10^{-3}$	$2.18\ 10^{-3}$
		$k_{2,i}$ $k^0_{2,i}$	$4.87\ 10^{-4}$	$2.46\ 10^{-3}$	$4.89\ 10^{-5}$	$1.59\ 10^{-3}$	$1.25\ 10^{-3}$
		$k_{2,i}$ $k^1_{2,i}$	$4.28\ 10^{-6}$	$8.91\ 10^{-4}$	$6.62\ 10^{-7}$	$1.57\ 10^{-6}$	$5.29\ 10^{-4}$
		$k_{2,i}$ $k^2_{2,i}$	---	$3.91\ 10^{-4}$	---	$2.47\ 10^{-3}$	$5.57\ 10^{-3}$
		$k_{3,i}$	0	0	0	0	$1.15\ 10^{-1}$
6.0	153	$k_{1,i}$	$2.30\ 10^{-3}$	$1.60\ 10^{-3}$	$3.01\ 10^{-4}$	$7.69\ 10^{-3}$	2.18 10-3
		$k_{2,i}$ $k^0_{2,i}$	$1.19\ 10^{-4}$	$8.38\ 10^{-6}$	0	0	$1.14\ 10^{-2}$
		$k_{2,i}$ $k^1_{2,i}$	$1.01\ 10^{-6}$	$1.58\ 10^{-6}$	$1.78\ 10^{-7}$	$3.50\ 10^{-6}$	$4.35\ 10^{-3}$
		$k_{2,i}$ $k^2_{2,i}$	---	$3.91\ 10^{-4}$	---	$5.41\ 10^{-4}$	0
		$k_{3,i}$	0	0	0	0	$1.15\ 10^{-1}$

4.2. Kinetic model of Fe release

When using the kinetic model by Martín-Torre et al. (2015b), the good fit between the experimental and simulated Fe release at pH values of 7.0 and 6.5 is shown in Fig. 8. Moreover, the Fe concentrations in the reduced and oxidised fractions, or $[FeRed]_0$ and $[FeOx]_0$, respectively, and the rate coefficients for the simulated Fe release at these pH values are listed in Table 5.

However, this model cannot explain the behaviour of Fe at the most acidic pH value under study. At pH=6.0, the simulated curves that employ this model explain the release of Fe within short periods but do not explain its decrease, nor is the second peak observed in Fe mobilisation (dashed curves in Fig. 8).

More complex kinetic schemes, which always consider first-order reactions with respect to Fe, have been tested to find a mathematical model that better predicts the behaviour of this element at pH=6.0. The possibility that Fe is released directly from the reduced fraction was considered; iron sulphides such as pyrite could be released into the medium without being oxidised. Another hypothesis was that most of the dissolved Fe precipitates took the form of Fe(III), whereas the rest of it precipitates as Fe(II) before being released again to the medium; afterwards, this re-dissolved Fe could precipitate as Fe(III). These kinetically Fe-dependent schemes do not improve the previous fitting, and so we propose that there is a dependency between the Fe release and the presence of other ions in association. Therefore, a model that includes the kinetics of ions associated with Fe is introduced. The global model of Fe consists of two series of reactions in parallel (Eqs. 11 and 12) and includes the influence of other ions on the release of Fe.

$$\mathrm{FeRed(s)} \xrightarrow{k_{1,Fe}} \mathrm{FeOx(s)} \xrightarrow{k_{2,Fe}} \mathrm{Fe^{2+}(aq)} \xrightarrow{k_{3,Fe}} \mathrm{Fe^{3+}(s)} \quad (11)$$

$$\mathrm{AC1(aq)} \xrightarrow{k_{1,a}} \mathrm{AS1(s)} \xrightarrow{k_{2,a}} \mathrm{AC2(aq)} \xrightarrow{k_{3,a}} \mathrm{AS2(s)} \quad (12)$$

Eq. 11 considers that reduced Fe should be oxidised before being released from the sediment into the medium, and that dissolved Fe precipitates as Fe(III) whereas Eq. 12 represents an additional scheme for ions that are associated with ~~to~~ Fe. Ions that are associated with Fe in solution (AC1) could precipitate with Fe (AS1) and be released together (AC2) and precipitated (AS2) because of the different solubility of products from the compounds present in the medium. This scheme is feasible because of the high concentration of ions dissolved in the seawater-sediment system and the ionic interactions associated with this situation.

The association between Fe and these ions is taken into account by assuming that the release and precipitation rate coefficients, namely $k_{2,Fe}$ and $k_{3,Fe}$, depend on the dissolved concentration of these ions through Eqs. 13 and 14.

$$k_{2,Fe} = {k^0}_{2,Fe} + {k^1}_{2,Fe}\, x_A \quad (13)$$

$$k_{3,Fe} = {k^0}_{3,Fe} + {k^1}_{3,Fe}\, (1 - x_A) \quad (14)$$

where ${k^0}_{2,Fe}$, ${k^1}_{2,Fe}$, ${k^0}_{3,Fe}$ and ${k^1}_{3,Fe}$ are kinetic rate coefficients and x_A is the fraction of ions released from the sediment, as calculated as $x_A = \frac{AC2 - AC1_0}{AC_{max}}$. AC2 refers to the concentration of ions released with Fe, $AC1_0$ is the concentration of seawater ions associated with Fe and AC_{max} is the maximum concentration of ions associated with Fe in the aqueous phase.

In Fig. 8, the simulated curves at pH=6.0 are shown using a continuous line. The proposed model fits well with the experimental data, including the second peak observed at the higher Fe concentrations in the selected seawater. The good fit is corroborated by the percentage variation-explained values (R^2) (99.3, 95.8 and 96.1 when the Fe concentrations of the seawater are 9.02, 46.1 and 153 µg/L, respectively). Additionally, Table 5 lists the maximum concentration of Fe that can be released from each fraction of the sediment and kinetic rate coefficients using the latter model.

This more complex model has been applied to the Fe release at pH values of 7.0 and 6.5 without obtaining an improvement in the simulated results. The global percentage variation-explained value of 97.8 and a relative standard deviation of 0.325 could be concluded for the Fe release model at the pH values and Fe seawater concentrations under study.

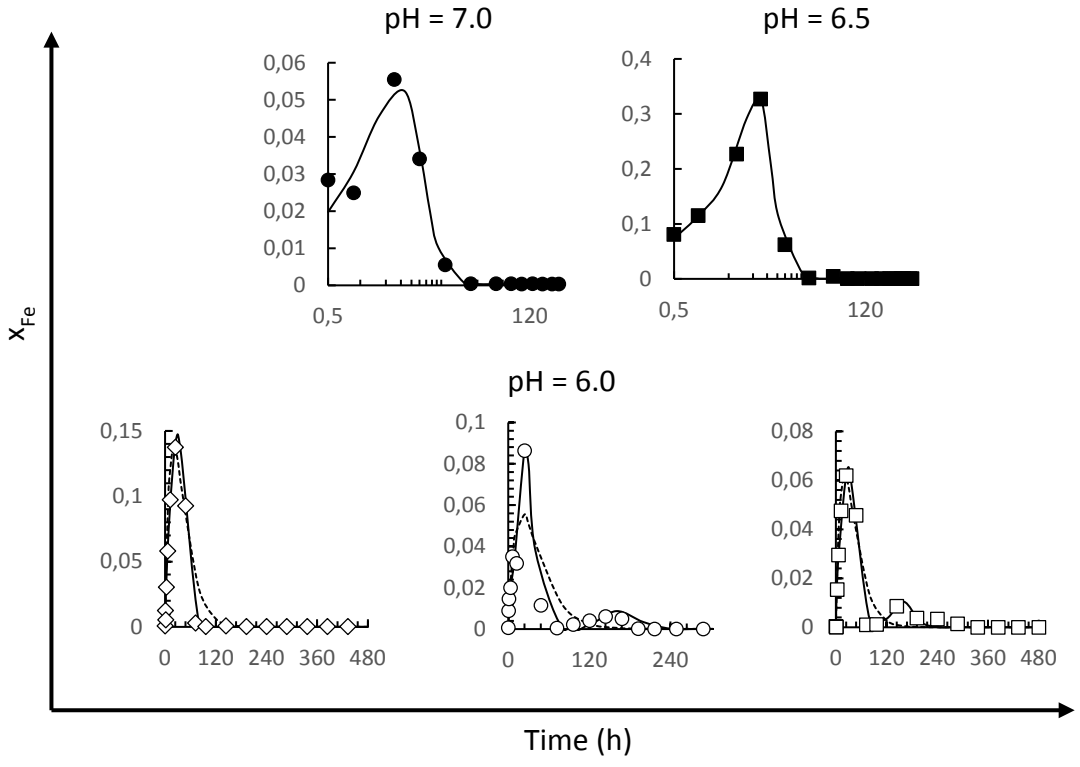

Fig. 8. Fe release ($x_{Fe} = [Fe]/[Fe]_0$) over time at pH values under study, where [Fe] is the dissolved concentration of Fe and $[FeS]_0$ is the maximum Fe concentration that can be released from the sediment. Experimental release (● pH=7; ■ pH=6.5; ◇pH=6.0, $[Fe]_{seawater}$=9.02 µg/L; ○ pH=6.0, $[Fe]_{seawater}$=46.1

µg/L; and □ pH=6.0, $[Fe]_{seawater}$=153 µg/L) and simulated curves are represented: ___most suitable model for each assay; - - -Martín-Torre et al. (2015b) model applied to assays at pH=6.0.

Table 5. Estimated values for the maximum concentrations of Fe that can be released from the reduced ($[FeRed]_0$) and oxidised ($[FeOx]_0$) sediment fractions and kinetic rate coefficients in all assays.

pH	$[Fe]_{seawater}$ (µg/L)	$[FeRed]_0$ (mg/kg)	$[FeOx]_0$ (mg/kg)	$k_{1,Fe}$ (h^{-1})	$k^0_{2,Fe}$ (h^{-1})	$k^1_{2,Fe}$ (h^{-1})	$k^0_{3,Fe}$ (h^{-1})	$k^1_{3,Fe}$ (h^{-1})	$k_{1,a}$ (h^{-1})	$k_{2,a}$ (h^{-1})	$k_{3,a}$ (h^{-1})
7.0	6.80	276	39.0	$1.08\ 10^{-4}$	$2.74\ 10^{-1}$	---	$2.95\ 10^{-1}$	---	---	---	---
6.5	3.50	86.0	623	$3.50\ 10^{-4}$	$2.01\ 10^{-1}$	---	$2.35\ 10^{-1}$	---	---	---	---
6.0	9.02	42.8	8040	$1.88\ 10^{-3}$	$1.42\ 10^{-2}$	$1.11\ 10^{-1}$	$9.73\ 10^{-2}$	0	$1.16\ 10^{-2}$	$1.15\ 10^{-2}$	$6.95\ 10^{-4}$
6.0	46.1	26.1	6620	$1.88\ 10^{-3}$	$1.09\ 10^{-2}$	$1.37\ 10^{-1}$	$1.32\ 10^{-1}$	$7.61\ 10^{-2}$	$1.71\ 10^{-2}$	$1.72\ 10^{-2}$	$1.62\ 10^{-3}$
6.0	153	58.6	18400	$1.88\ 10^{-3}$	$9.90\ 10^{-3}$	$4.12\ 10^{-2}$	$1.69\ 10^{-1}$	$6.80\ 10^{-2}$	$1.89\ 10^{-2}$	$1.89\ 10^{-2}$	$1.52\ 10^{-3}$

612 **4.3. Trace element modelling at pH=6.0**

613 The contaminant release at pH=6.0 is first simulated according to the kinetic scheme
614 used at higher pH values (Eq. 3). However, the release reaction is influenced by the
615 dissolved Fe concentration so the rate coefficient $k_{2,i}$ is modified according to Eq. 15 to
616 account for this effect.

$$k_{2,i} = {k^0}_{2,i} + \frac{{k^1}_{2,i}}{x_{Fe}} \quad (15)$$

617

618 where i represents the element (Zn, Pb, Ni, Cd, or As), ${k^0}_{2,i}$ and ${k^1}_{2,i}$ are kinetic rate
619 coefficients, whereas the fraction of Fe released from the sediment is defined as $x_{Fe} =$
620 $\frac{[Fe]}{[FeS]_0}$ with [Fe] being the dissolved concentration of Fe and $[FeS]_0$ being the maximum
621 concentration of Fe that can be released from the sediment. The former coefficient
622 (${k^0}_{2,i}$) considers the characteristics of the aqueous medium that might modify the
623 solubility of the different species present in the sediment whereas ${k^1}_{2,i}$ represents the
624 direct influence of Fe on the release rate.

625

626 Including the influence of Fe, the simulated results of Zn and Cd fit well with their
627 experimental release. However, the simulated release of Pb, Ni and As (not shown) is
628 much lower than the experimental one for short periods (t<96 h) so the ionic
629 competition with other cations should be considered in a similar way as the Fe release.

630

631 To avoid a high increase in the number of parameters, only the influence of Zn, which is
632 the major trace element in the studied sediment, is also included when simulating the
633 release of Pb, Ni and As. Hence, a further term is added and the rate coefficient of the

634 release reaction of Pb, Ni and As includes the combined influence of Fe and Zn as
635 shown in Eq. 16.

$$k_{2,i} = {k^0}_{2,i} + \frac{{k^1}_{2,i}}{x_{Fe}} + \frac{{k^2}_{2,i}}{x_{Zn}} \quad (16)$$

636

637 where i represents the element (Pb, Ni and As), ${k^2}_{2,i}$ is the rate coefficient which
638 represents the direct influence of Zn on the release rate and the fraction of Zn released
639 from the sediment is defined as $x_{Zn} = \frac{[Zn]}{[ZnS]_0}$ with [Zn] being the concentration of
640 dissolved Zn and $[ZnS]_0$ being the maximum concentration of Zn that can be released
641 from the sediment. The variables ${k^0}_{2,i}$, ${k^1}_{2,i}$ and x_{Fe} were previously explained.

642

643 The fit between the simulated and experimental release for the different assays at
644 pH=6.0 when using this modified model is shown in Fig. 7 with continuous lines. The
645 percentage variation-explained values values (R^2) for the different assays at pH=6.0 are,
646 from the lowest to the highest concentrations of Fe in the seawater, 99.5, 96.1 and 96.3.
647 These values are influenced by the simulated release of Fe, leading to higher R^2 values
648 of elemental release for the better Fe fittings.

649

650 The concentrations of each element in the reduced and oxidised sediment fractions are
651 estimated by using this modified model and are listed in Table 3. At pH=6 and
652 $[Fe]_{seawater}$=9.02 µg/L, the estimated concentrations take the same value as they do when
653 using the model by Martín-Torre et al. (2015b). Similar to what occurred at most neutral
654 pH values, higher concentrations are released from the reduced fraction than from the
655 oxidised fraction of the sediment, except the Ni and As in the assay in which the
656 seawater contains 46.1 µg/L of Fe.

Regarding the pH=6 assay with the lowest seawater Fe concentration (9.02 µg/L), a better fitting is obtained when using the modified model than the previous one. Percentage variation-explained values (R^2) of 99.5, 98.6, 99.7, 98.4 and 81.2 instead of 99.3, 98.4, 98.3, 97.0 and 74.1 are obtained for Zn, Pb, Cd, Ni and As, respectively. However, a trade-off between the estimated work and the accuracy should be decided by the user because the use of this modified model implies the estimation of more parameters.

Given that ionic competition~~,~~ based on the different solubility products~~,~~ is a process with a great influence on the contaminant release, the interactions among all of the ions could be added through additional elemental fractions (x_{Pb}, x_{Cd}, x_{Ni} and x_{As}). This approach has been attempted, and despite the increasing the number of estimated parameters, the results do not present enough sensitivity to better fit the experimental release. Hence, the dependence of Fe is considered for all the studied trace elements at pH=6.0, but the influence of Zn is only contemplated for Pb, Ni and As release at this pH value.

Something similar occurs when this model, which was proposed for the simulation of contaminant release at pH=6.0, is used to fit experimental results from assays at pH values of 7.0 and 6.5 a better fit is obtained when the parameters that are not included in the initial proposed model employ a value of zero.

As expected, higher concentrations of the studied trace elements are released from the sediment ($[MS]_{i,0} = [MOx]_{i,0} + [MRed]_{i,0}$) at lower pH values because of the greater

solubility of the studied contaminants at acidic pH values, except for As, which presents the highest mobilisation at pH=6.5 (Fig. 9 a). In comparing the mobilisation at pH=6.0, Fig. 9b indicates that the higher Fe concentrations in the selected seawater causes a slightly higher mobilisation of all the studied contaminants.

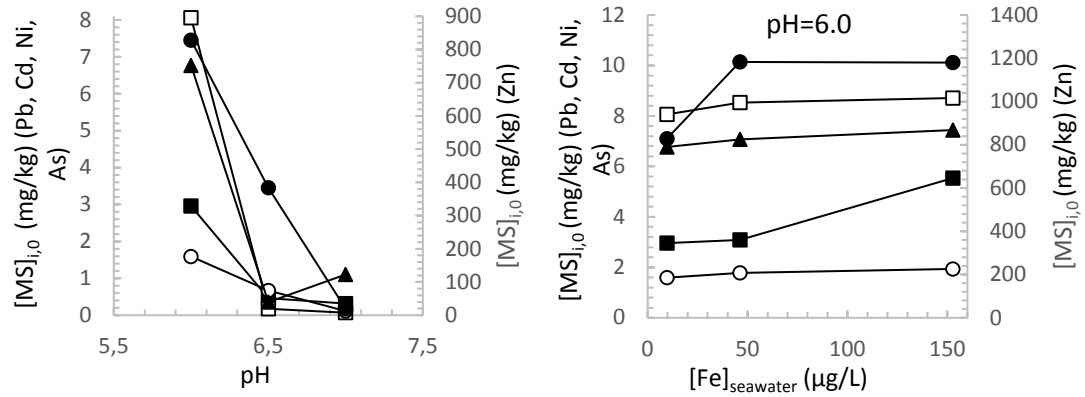

a) b)

Fig. 9. a) Maximum concentration of contaminant that can be released from the sediment as a function of pH; and b) maximum concentration of contaminant that can be released from the sediment at pH=6.0 as a function of the Fe concentration in the seawater. ● Zn; ■ Pb; ○ Ni; □ Cd; and ▲ As

As previously stated, the rate coefficients of the different assays are presented in Table 4, in which As is the only element with an adsorption or precipitation reaction ($k_3 \neq 0$). Moreover, at pH=6.0 the oxidation and adsorption/precipitation processes of this oxyanion do not depend on the initial Fe concentration in the seawater, and thus the rate coefficients have the same value in the three assays conducted at this pH value.

Although the model considers the influence of Zn on the release of Pb, Ni and As, it takes a nonzero value ($k^2_{2,i} \neq 0$) in all the cases for Ni release, for Pb release at the two highest concentrations of Fe in seawater (153 and 46.1 µg/L) and for As mobilisation at $[Fe]_{seawater}$= 46.1 µg/L; this last case likely occurs because the released concentration of this oxyanion from the oxidised fraction is higher than it was from the reduced fraction

704 at this seawater Fe content. However, the obtained rate kinetic parameters ($k^0_{2,i}$, $k^1_{2,i}$
705 and $k^2_{2,i}$) do not present a clear trend as a function of $[Fe]_{seawater}$.
706
707 The type of acidification (CO_2 or HNO_3) used in the pH-static assay influences the rate
708 coefficients obtained from the Martín-Torre et al. model (2015b). Contrary to what
709 occurs when the mineral acid is used (Martín-Torre et al., 2015b), rate coefficients
710 obtained using CO_2 do not present a clear trend with respect to the pH and cannot be
711 fitted to any polynomial equation. HNO_3 is a strong oxidising acid that generates
712 soluble salts in the medium, and it might be completely dissociated. CO_2 is a weak
713 oxidising acid that forms partial insoluble salts, the solubility products of which modify
714 the characteristics of the medium through ionic competition and therefore influence the
715 element release rates.
716
717 The maximum concentrations of the elements that can be released from the sediment
718 might depend on the type of acidification in addition to the oxidation state of the
719 sediment. Hence, higher values are generally obtained in assays that employ CO_2
720 instead of HNO_3 (Martín-Torre et al., 2015b). Exceptions to this trend are Pb
721 concentration at pH values of 7.0 and 6.5 (similar values are independent of the selected
722 acid) and As at the most neutral pH values, where higher concentrations are released
723 from the sediment in assay samples acidified by HNO_3.
724
725 The parity plots with the percentage variation-explained values (R^2) and relative
726 standard deviation (RSD) included a consideration of the global modified model of this
727 work for all the assays performed, as obtained for each contaminant (Fig. 10). Parity
728 plots are useful for the validation of the model in terms of the released element

729 concentration at any time and pH value. In general, at release higher than 25% of the
730 maximum dissolved concentration, differences between experimental and simulated
731 mobilisation are lower than 20% although a higher dispersion is observed in the case of
732 As. Better fittings are obtained at pH values of 7.0 and 6.5 because of a lack of ~~the~~
733 influence from the Fe concentration and ionic competition on the elemental release. The
734 percentage variation-explained values (R^2) for each contaminant are higher than 97.8 for
735 all the elements under study, except for As, in which R^2=89.4. The high values of this
736 statistical parameter show the good fit of the proposed model.

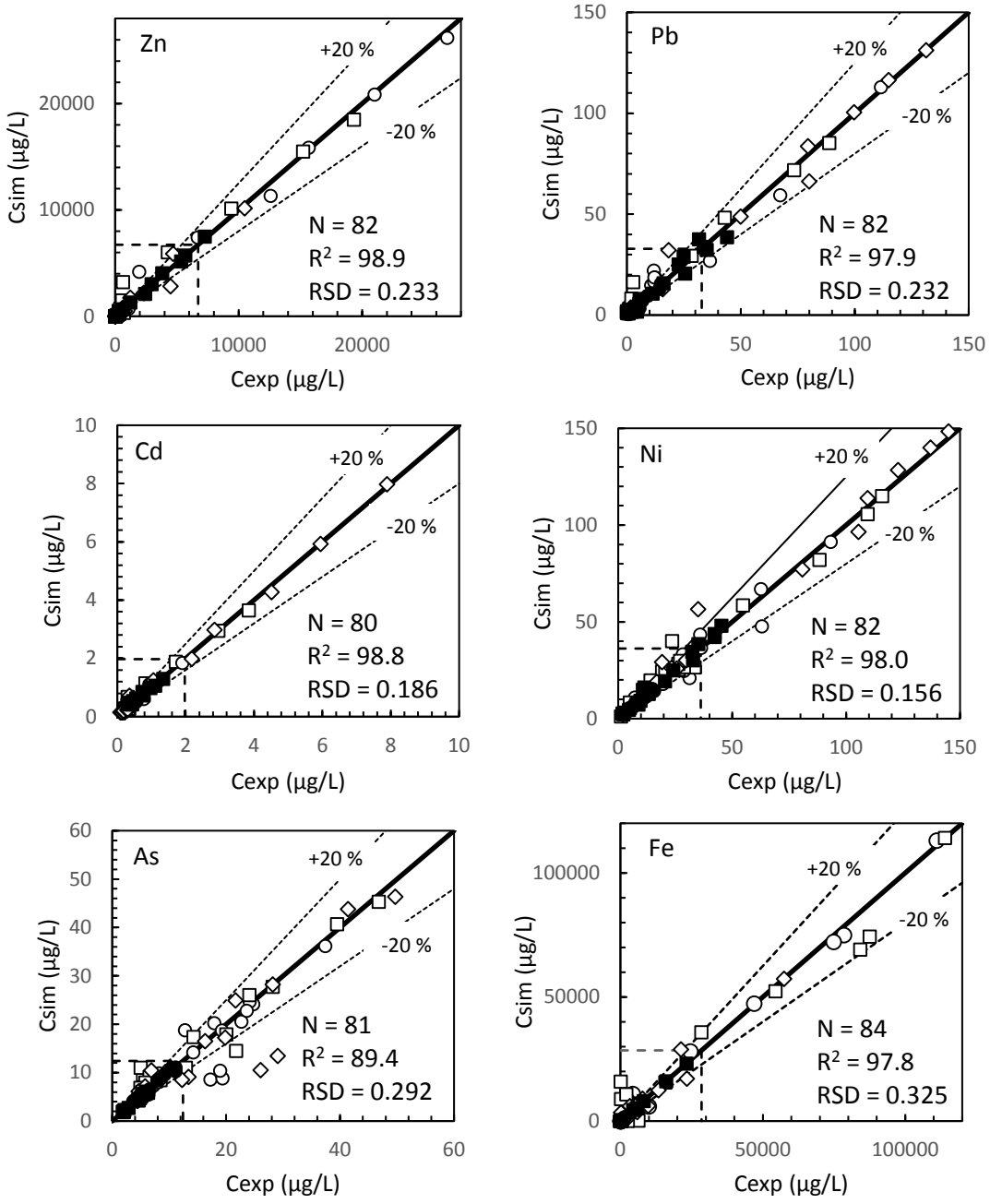

737

738

739

740

741 Fig. 10. Parity plots of the element concentrations from the experiment (Cexp) and simulated results
742 (Csim) of the elements under study. The area inside the dashed square includes concentrations lower than
743 25% of the maximum dissolved concentration. ● pH=7.0; ■ pH=6.5; ◇pH=6.0, $[Fe]_{seawater}$=9.02 µg/L; ○
744 pH=6.0, $[Fe]_{seawater}$=46.1 µg/L; and □ pH=6.0, $[Fe]_{seawater}$=153 µg/L. Additionally, the data number (N),
745 percentage variation-explained value (R^2) and relative standard deviation (RSD) are shown.

746

747 **5. CONCLUSIONS**

748 This work presents the experimental results of Zn, Pb, Cd, Ni, Cr, Cu and As
749 mobilisation over time when sediment and seawater are totally mixed and acidified by

CO_2 gas in a pH-static leaching test. Long-term 480-h leaching tests are performed at pH values of 7.0, 6.5 and 6.0 to assess different levels of acidification.

The evolution of the redox potential and Fe release over time at pH=6.0 is different than the evolution at the more neutral pH values under study. Therefore the influence of the seawater Fe concentration is assessed by conducting assays at pH=6.0 using natural seawater with different Fe contents: 9.02; 46.1 and 153 μg/L.

A set of three in-series reactions for trace elements, for Fe and for other ions associated with Fe is proposed to model a Fe/multi-ion-dependent mechanism for trace metal release. The model uses global R^2 values of 98.9-89.4 and RSD < 0.325 to explain the release behaviour over time for Zn, Pb, Cd, Ni and As at pH values of 7.0, 6.5 and 6.0, which mimic the potential CCS acidification, and three seawater iron concentrations, which represent estuarine seawater in the iron mine areas.

The model proposed in this work extends the scope of previous models to the acidification of seawater with CO_2, at different iron concentrations; however, a trade-off between estimation and accuracy is made because there are higher numbers of parameters in the proposed model. Using the Aspen Custom Modeler, the maximum concentrations of each element that can be released from the sediment, and the kinetic rate coefficients are estimated for all the cases.

Additionally, the kinetic rate coefficients obtained in this work are compared with those that were obtained previously when HNO_3 was used to acidify the medium. Different trends are observed because of the impact that CO_2 has on the ionic competition and

contaminant release, highlighting that the displacement reactions should be considered when acidification from CO_2 leakages originating from CCS sites is assessed.

The parity plots of the pH-static leaching test when using CO_2 to acidify the medium show a good fit between the experimental and simulated element release, confirming that the proposed model can be applied to simulate contaminant mobilisation from contaminated sediment to seawater under total mixed acidic conditions at pH values of 7.0, 6.5 and 6.0. Hence, a useful, broader generalised kinetic model that explains the contaminant release over time in sediment-seawater mixtures that were acidified by HNO_3 or CO_2 was made to obtain acidic pH values and different concentrations of iron. The proposed model is flexible enough to work with sediments that have different contaminant contents through model-fitting parameters such as the oxidised and reduced fractions and the kinetic rate coefficients.

Acknowledgements

This work was financially supported by the Spanish Ministry of Economy and Competitiveness, Project CTM 2011-28437-C02-01, ERDF included. M.C. Martín-Torre was funded by the Spanish Ministry of Economy and Competitiveness by means of F.P.I. fellowship No. BES-2012-053816.

References

Appelo, C.A.J., Drijver, B., Hekkenber, R., de Jonge, M. 1999. Modeling in situ iron removal from groundwater. Groundwater 37 (6), 811-817.

Appelo, C. A. J., van der Weiden, M. J. J., Tournassat, C, Charlet, L. 2002. Surface complexation of ferrous iron and carbonate on ferrihydrite and the mobilization of arsenic. Environ. Sci. Technol., 36, 3096-3103. DOI: 10.1021/es010130n

Arai, Y., Sparks, D. L., Davis, J.A. 2004. Effects of dissolved carbonate on arsenate adsorption and surface speciation at the hematite-water interface. Environ. Sci. Technol. 2004, 38, 817-824. DOI: 10.1021/es034800w

Ardelan, M. V., Steinnes, E., Lierhagen, S., Linde, S. O. 2009. Effects of experimental CO2 leakage on solubility and transport of seven trace metals in seawater and sediment. Sci. Total Environ. 407 (24), 6255-6266. DOI: 10.1016/j.scitotenv.2009.09.004

Ardelan, M. V., Steinnes, E. 2010. Changes in mobility and solubility of the redox sensitive metals Fe, Mn and Co at the seawater-sediment interface following CO2 seepage. Biogeosciences, 7, 569–583. DOI: 10.5194/bg-7-569-2010

Basallote, M.D., de Orte, M.R., del Valls, T.A., Riba, I. 2014. Studying the effect of CO_2-induced acidifciation on sediment toxicity using acute amphipod toxicity test. Environ. Sci. Technol. 48, 8864-8872. DOI: 10.1021/es5015373

Bateman, K., Turner, G., Pearce, J.M., Noy, D. J., Birchall, D., Rochelle, C. A. 2005. Large-Scale Column Experiment: Study of CO_2, porewater, rock reactions and model test case. Oil Gas Sci. Technol., Vol. 60 (1), 161-175.

BOE, 2008. Resolution of 28 November 2007, vol. 34. Spanish Ministry of Industry, Tourism and Trade, Madrid, Spain, pp. 7099-7102.

Cahill, A. G. and Jakobsen, R. 2015. Geochemical modeling of a sustained shallow aquifer CO2 leakage field study and implications for leakage and site monitoring. Int. J. Greenh. Gas Con. 37, 127–141. DOI: 10.1016/j.ijggc.2015.03.011

Cappuyns, V., Swennen, R. and Verhulst, J. 2004a. Assessment of acid neutralizing capacity and potential mobilisation of trace metals from land-disposed dredged sediments. Science of the Total Environment, 333 (1-3), 233- 247. DOI: 10.1016/j.scitotenv.2004.05.007

Cappuyns, V., Swennen, R. and Devivier, A. 2004b. Influence of ripening on pH_{stat} leaching behaviour of heavy metals from dredged sediments. Journal of Environmental Monitoring 6 (9), 774-781. DOI: 10.1039/B406672C

Cappuyns, V., Swennen, R. 2005. Kinetics of element release during combined oxidation and pHstat leaching of anoxic river sediments. Appl. Geochem. 20, 1169–1179. DOI : 10.1016/j.apgeochem.2005.02.004

Cappuyns, V. and Swennen, R. 2008. The application of pHstat leaching tests to assess the pH-dependent release of trace metals from soils, sediments and waste materials. J. Hazard. Mater. 158(1), 185-195. DOI: 10.1016/j.jhazmat.2008.01.058

CEN/TS 14997. 2015. Characterization of waste - Leaching behaviour tests – Influence of pH on leaching with continuous pH-control.

Centioli, D., Comans, R.N.J., Gaudino, S., Galas, C., Belli, M. 2008. Leaching tests: useful tools for the risk assessment of contaminated sediments. Annali dell'Istituto Superiore di Sanità 44 (3), 252-257.

Coz, A., González-Piñuela, C., Andrés, A., Viguri, J.R. 2007. Physico-chemical and environmental characterisation of sediments from Cantabria estuaries (Northern Spain). Aquat. Ecosyst. Health, 10, 41-46. DOI: 10.1080/14634980701212118

De Orte, M. R., Sarmiento, A. M., Basallote, M. D., Rodríguez-Romero, A., Riba, I., del Vallas, A. 2014. Effects on the mobility of metals from acidification caused by possible CO2 leakage from sub-seabed geological formations. Sci. Total Environ. 470-471, 356-363. DOI: 10.1016/j.scitotenv.2013.09.095

Di Toro, D., Mahony, J. D., Hansen, D. J., Scott, K. J., Hicks, M. B., Mayr, S. M., Redmond, M. 1990. Toxicity of cadmium in sediments: the role of acid volatile sulfide. Environ. Toxicol. Chem. 9, 1487–1502. DOI: 10.1002/etc.5620091208

Eggleton, J. and Thomas, K.V. 2004. A review of factors affecting the release and bioavailability of contaminants during sediment disturbance events. Environ. Int.. 30(7), 973-980. DOI: 10.1016/j.envint.2004.03.001

Frye, E., Bao, C., Li, L., Blumsack, S. 2012. Environmental Controls of Cadmium Desorption during CO2 Leakage. Environ. Sci. Technol., 46, 4388−4395. DOI: 10.1021/es3005199

Hering, J. G. and Stumm, W. 1990. Oxidative and reductive dissolution of minerals. In Mineral-Water Interface Chemistry, vol. 23 (eds. M. F. Hochella and A. F. White), 427–465. Reviews in Mineralogy and Geochemistry. Mineralogical Society of America.

Hoffman, E.L. 1992. Instrumental neutron activation in geoanalysis. J. geochem. Explor. 44, 297-319. DOI: 10.1016/0375-6742(92)90053-B

Horckmans, L., Swennen, R., Deckers, J. 2007. Retention and release of Zn and Cd in spodic horizons as determined by pHstat analysis and single extractions. Sci Total Environ. 376, 86–99. DOI: 10.1016/j.scitotenv.2007.01.077

Hwang, K.-Y., Kim, H.-S., and Hwang, I. 2011. Effect of Resuspension on the Release of Heavy Metals and Water Chemistry in Anoxic and Oxic Sediments. Clean – Soil, Air, Water 39 (10), 908–915. DOI: 10.1002/clen.201000417

Intergovernmental Panel on Climate Change (IPCC) (2014) Climate change 2014: mitigation of climate change. In: Working Group III of the Intergovernmental Panel on Climate Change.

Ishimatsu, A., Kikkawa, T., Hayashi, M., Lee, K.-S., Kita, J. 2004. Effects of CO2 on marine fish: larvae and adults. J. oceanogr. 60, 731-741. DOI: 10.1007/s10872-004-5765-y

Jain, A., Loeppert, R.H. 2000. Effect of competing anions on the adsorption of arsenate and arsenite by ferrihydrite. J. Environ. Qual. 29 (5), 1422–1430.DOI: 10.2134/jeq2000.00472425002900050008x

Johnston, S.G. , Morgan, B., Burton, E.D. 2016. Legacy impacts of acid sulfate soil runoff on mangrove sediments: Reactive iron accumulation, altered sulfur cycling and trace metal enrichment. Chem. Geol. 427 (1), 43–53. DOI: 10.1016/j.chemgeo.2016.02.013

908 Kikkawa, T., Kita, J. and Ishimatsu, A. 2004. Comparison of the lethal effect of CO2
909 and acidification on red sea bream (Pagrus major) during the early developmental
910 stages. Mar. Pollut. Bull. 48, 108–110. DOI: 10.1016/S0025-326X(03)00367-9
911
912 Kirsch, K., Navarre-Sitchler, A. K., Wunsch, A., McCray, J. E. 2014. Metal Release
913 from Sandstones under Experimentally and Numerically Simulated CO2 Leakage
914 Conditions. Environ. Sci. Technol. 48, 1436−1442. DOI: 10.1021/es403077b
915
916 Lawter, A., Qafoku, N. P., Wang, G., Shao, H., Brown, C. F. 2016. Evaluationg impacts
917 of CO2 intrusion into an unconsolidated aquifer: I. Experimental data. Int. J. Greenh.
918 Gas Con. 44, 323-333. DOI: 10.1016/j.ijggc.2015.07.009
919
920 Little, M.G., Jackson, R.B. 2010. Potential impacts of leakage from deep CO2
921 geosequestration on overlying freshwater aquifers. Environ. Sci. Technol., 44, 9225–
922 9232. DOI: 10.1021/es102235w
923
924 Lu, J., Partin, J. W., Hovorka, S. D., Wong, C. 2010. Potential risks to freshwater
925 resources as a result of leak-age from CO2 geological storage: a batch-reaction
926 experiment. Environ. Earth Sci. 60 (2), 335–348. DOI: 10.1007/s12665-009-0382-0
927
928 Luther III, G.W., Kostka, J.E., Church, T.M., Sulzberger, B., Stumm, W. 1992.
929 Seasonal iron cycling in the salt-marsh sedimentary environment: the importance of
930 ligand compelxes with Fe(II) and Fe(III) in the dissolution of Fe(III) minerals and
931 pyrite, respectively. Mar. Chem. 40, 81-103. DOI: 10.1016/0304-4203(92)90049-G
932
933 Martín-Torre, M.C., Payán, M.C., Verbinnen, B., Coz, A., Ruiz, G., Vandecasteele, C.,
934 Viguri, J.R. 2015a. Metal release from contaminated estuarine sediment under pH
935 changes in the marine environment. Arch. Environ. Contam. Toxicol. 68(3), 577–587.
936 DOI: 10.1007/s00244-015-0133-z
937
938 Martín-Torre, M.C., Ruiz, G., Galán, B., Viguri, J.R. 2015b. Generalised mathematical
939 model to estimate Zn, Pb, Cd, Ni, Cu, Cr and As release from contaminated estuarine
940 sediment using pH-static leaching tests. Chem. Eng. Sci. 138, 780-790. DOI:
941 10.1016/j.ces.2015.08.053
942
943 Meng, X.G., Bang, S.B., Korfiatis, G.P. 2000. Effects of silicate, sulfate, and carbonate
944 on arsenic removal by ferric chloride. Water Res. 34, 1255–1261. DOI: 10.1016/S0043-
945 1354(99)00272-9
946
947 Meng, X., Korfiatis, G.P., Bang, S., Bang, K. 2002. Combined effects of anions on
948 arsenic removal by iron hydroxides. Toxicol. Lett. 113, 103–111. DOI: 10.1016/S0378-
949 4274(02)00080-2
950
951 Millero, F.J., Sotolongo, S., Izaguirre, M. 1987. The oxidation kinetics of Fe(II) in
952 seawater. Geochim. Cosmochim. Ac. 51, 793-801.
953
954 Millero, F.J. and Izaguirre, M. 1989. Effect of ionic strength and ionic interactions on
955 the oxidation of Fe(II). J. Solution Chem. 18 (6), 585-599.
956

957 Millero, F. J., Yao, W. and Aicher, J. 1995. The speciation of Fe(II) and Fe(III) in
958 natural waters. Mar. Chem. 50 (1-4), 21–39. DOI: 10.1016/0304-4203(95)00024-L
959
960 Millero, F. J. 2009. Thermodynamic and Kinetic Properties of Natural Brines. Aquat.
961 Geochem. 15 (1), 7-41. DOI: 10.1007/s10498-008-9053-0
962
963 Morse, J. W. and Arakaki, T. 1993. Adsorption and coprecipitation of divalent metals
964 with mackinawite (FeS). Geochim. Cosmochim. Ac. 57 (15), 3635-3640. DOI:
965 10.1016/0016-7037(93)90145-M
966
967 Omoregie, E. O., Couture, R.-M., van Cappellen, P., Corkhill, C. L., Charnock, J. M.,
968 Polya, D. A., Vaugahn, D., Vanbroekhoven, K., Lloyd, J. R. 2013. Arsenic
969 Bioremediation by Biogenic Iron Oxides and Sulfides. Appl. Environ. Microb. 79 (14),
970 4325-4335. DOI: 10.1128/AEM.00683-13
971
972 Payán, M.C., Galan, B., Coz, A., Vandecasteele, C., Viguri, J.R. 2012a. Evaluation
973 through column leaching tests of metal release from contaminated estuarine sediment
974 subject to CO_2 leakages from Carbon Capture and Storage sites. Environ. Pollut. 171,
975 174-184. DOI:10.1016/j.envpol.2012.07.029
976
977 Payán, M.C., Verbinnen, B., Galan, B., Coz, A., Vandecasteele, C., Viguri, J.R., 2012b.
978 Potential influence of CO2 release from a carbon capture storage site on release of trace
979 metals from marine sediment. Environ. Pollut. 162, 29–39. DOI:
980 10.1016/j.envpol.2011.10.015
981
982 Payán, M.C., Galan, B., Ruiz, G., Coz, A., Viguri, J.R. 2013. Pb and Zn release from
983 intertidal marine sediment in contact with acidified CO2 seawater: Mathematical model
984 for column leaching tests. Chem. Eng. Sci. 95, 85–93. DOI: 10.1016/j.ces.2013.02.059
985
986 Rodríguez-Romero, A., Basallote, M. D., De Orte, M. R., Delvalls, T. Á., Riba, I.,
987 Blasco, J. 2014. Simulation of CO_2 leakages during injection and storage in sub-seabed
988 geological formations: Metal mobilization and biota effects. Environ. Int. 68, 105−117.
989 DOI: 10.1016/j.envint.2014.03.008
990
991 Root, R.A., Dixit, S., Campbell, K. M., Jew, A.D., Hering, J. G. and O'Day, P.A. 2007.
992 Arsenic sequestration by sorption processes in high-iron sediments. Geochim.
993 Cosmochim. Ac. 71, 5782-5803. DOI: 10.1016/j.gca.2007.04.038
994
995 Salomons, W. 1995. Long-term strategies for handling contaminated sites and large-
996 scale areas. In: Salomons, W. and Stigliani, W. M. (Eds.), Biogeodynamics of
997 Pollutants in Soils and Sediments (Risk assessment of delayed and non-linear
998 responses), Springer, Berlín (Germany), 1-30. ISBN: 3-530-58732-2
999
1000 Schwertmann, U. 1991. Solubility and dissolution of iron oxides. Plant Soil 130 (1), 1–
1001 25.
1002
1003 Shtiza, A., Swennen, R., Cappuyns, V., Tashko, A. 2009. ANC, BNC and mobilization
1004 of Cr from polluted sediments in function of pH changes. Environ. Geol. 56(8), 1663-
1005 1678. DOI: 10.1007/s00254-008-1263-7
1006

Sigg, L. 2000. Redox potential measurements in natural waters: significance, concepts and problems. In:Schulz, H.D., Fischer, W.R., Böttcher, J., Duijnisveld, W.H.M. (Eds.), Redox Fundamentals, Processes and Applications. Springer, Berlin, pp. 1–12.

Thamdrup, B. 2000. Bacterial manganese and iron reduction in aquatic systems. Adv. Microb. Ecol. 16, 41–84.

Tokoro, C., Yatsugi, Y., Koga, H., Owada, S. 2010. Sorption Mechanisms of Arsenate during Coprecipitation with Ferrihydrite in Aqueous Solution. Environ. Sci. Technol. 44 (2), 638–643. DOI: 10.1021/es902284c

Vaca-Escobar, K., Villalobos, M., Pi-Puig, T., Zanella, R. 2015. Approaching the geochemical complexity of As(V)-contaminated systems through thermodynamic modelling Chem. Geol. 410, 162–173. DOI: 10.1016/j.chemgeo.2015.06.007

Wallmann, K., Petersen, W., Reiners, C, Gramm, H. 1996. Trace element diagenesis in polluted sediments of the river Elbe estuary. In: Calmano, W. and Förstner, U. (Eds.), Sediments and toxic substances (Environmental effects and ecotoxicity), Berlín (Germany), 197-213. ISBN: 3-540-60051-5

Van Herreweghe, S., Swennen, R., Cappuyns, V., Vandecasteele, C. 2002. Chemical associations of heavy metals and metalloids in contaminated soils near former ore treatment plants: a differentiated approach with emphasis on pH_{stat}-leaching. J. Geochem. Explor. 76 (2), 113– 138. DOI: 10.1016/S0375-6742(02)00232-7

Wang, G., Qafoku, N.P., Lawer, A.R., Bowden, M., Harvey, O., Sullivan, C., Brown, C.F. 2016. Geochemical impacts of leaking CO2 from subsurface storage reservoirs to an unconfined oxidizing carbonate aquifer. Int. J. Greenh. Gas. Con. 44,310–322.DOI: 10.1016/j.ijggc.2015.07.002

Wong, V.N., Johnston, S.G., Burton, E.D. Bush, R.T, Sullivan, L.A., Slavich, P.G. 2013. Seawater-induced mobilization of trace metals from mackinawite-rich estuarine sediments. Water Res. 47(2):821-32. DOI: 10.1016/j.watres.2012.11.009

Zhang, G.-S., Qu, J.-H., Liu, H.-J., Liu, R.-P., Li, G.-T. 2007. Removal Mechanism of As(III) by a Novel Fe−Mn Binary Oxide Adsorbent: Oxidation and Sorption. Environ. Sci. Technol. 41 (13), 4613–4619. DOI: 10.1021/es063010u

Zheng, L., Apps, J. A., Zhang, Y., Xu, T., Birkholzer, J. T. 2009. On mobilization of lead and arsenic in groundwater in response to CO2 leakage from deep geological storage. Chem. Geol. 268, 281–297. DOI: 10.1016/j.chemgeo.2009.09.007

Zheng, L., Qafoku, N. P., Lawter, A., Wang, G., Shao, H., Brown, C. F. 2016. Evaluating impacts of CO2intrusion into an unconsolidated aquifer: II.Modeling results. Int. J. Greenh. Gas Con. 44, 300–309. DOI: 10.1016/j.ijggc.2015.07.001